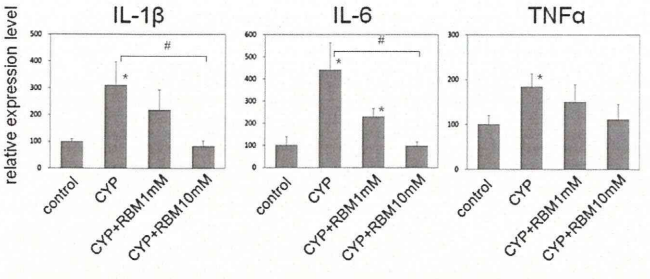

Figure 3. mRNA levels of proinflammatory cytokines IL-1β, IL-6 and TNF-α were compared with GAPDH level by real-time reverse transcriptase-polymerase chain reaction. Trends similar to those of MPO expression were observed. Asterisk indicates $p < 0.05$ vs control. Pound sign indicates $p < 0.05$ between groups.

dose dependently reversed the ICI decrease with no significant difference between the control and rebamipide treated groups (see table and fig. 4). Baseline pressure, voiding pressure thresholds and peak voiding pressure did not differ among the groups.

DISCUSSION

CYP administered in the peritoneum is transformed to its metabolite acrolein, which is excreted in urine and injures the urinary tract. CYP treated rats show frequent micturition[12] and bladder inflammation, as evidenced by proinflammatory cytokine increase and multimorphological inflammatory cell infiltration.[13] As reported previously, bladder inflammation increases afferent sensitivity and nociception.[12,14]

Our results show that intravesical application of rebamipide suppressed bladder inflammation and bladder overactivity in the chemically induced cystitis rat model. We speculate that the mechanism of improvement of bladder overactivity by rebamipide is due to the suppression of inflammation, leading to decreased visceral pain. Previous groups reported that rebamipide suppresses inflammation in many organs.[1,3,5–8,10,11,15] To our knowledge this is the first report demonstrating the efficacy of rebamipide for bladder inflammation.

Cystometrogram parameters

	Mean ± SE Pressure (cm H_2O)			Mean ± SE ICI (mins)
	Baseline	Threshold	Peak	
Control	7.0 ± 0.8	11.3 ± 1.0	30.2 ± 2.6	22.4 ± 2.3
CYP (+ mM rebamipide) :	8.7 ± 1.7	12.5 ± 0.9	28.8 ± 3.0	10.7 ± 0.7*
1	7.1 ± 0.6	10.7 ± 0.8	29.6 ± 1.8	14.4 ± 2.1†
10	8.3 ± 1.7	13.5 ± 1.0	31.3 ± 3.9	21.1 ± 2.5‡

* $p < 0.01$ vs control.
† $p < 0.05$ vs control.
‡ $p < 0.01$ vs CYP.

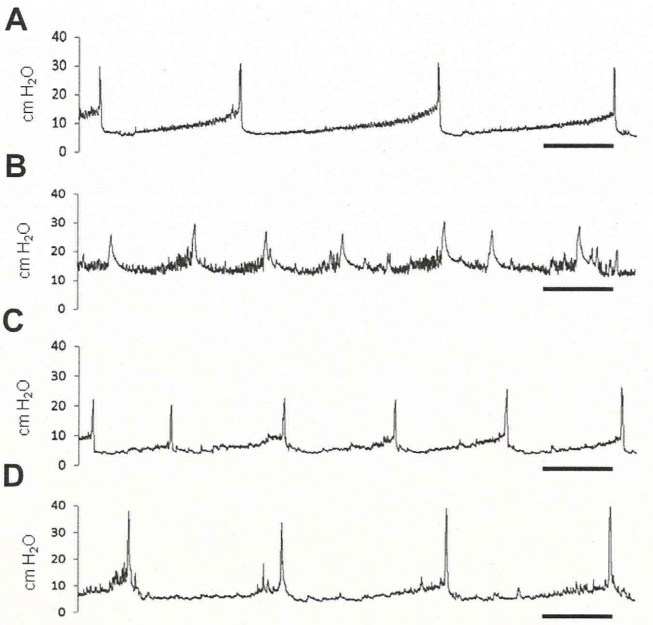

Figure 4. Cystometrogram shows representative intravesical pressure in controls (*A*), and rats treated with CYP (*B*), CYP plus 1 mM rebamipide (*C*) and CYP plus 10 mM rebamipide (*D*). ICI during cystometrogram was significantly less in CYP treated rats. Rebamipide prolonged micturition interval in dose dependent manner. Bar indicates 10 minutes.

The urine volume of rats is reportedly 7 to 10 ml per day (300 to 500 μl per hour). Therefore, instilled rebamipide would be diluted by almost half, although 10 mM rebamipide effectively suppressed bladder inflammation.

Many studies have been done to determine the mechanism of action of rebamipide. It involves the inhibition of inflammatory cytokines and inflammatory cell infiltration, suppression of neutrophil function, scavenging of oxygen free radicals, increased mucous secretion, stabilization of the mucosal barrier and enhanced generation of endogenous prostaglandins.[1–3,6–8,15–17] Sakurai et al examined the effect of oral intake of rebamipide on neutrophil infiltration using acetic acid induced gastric ulcers in rats.[17] Although they noted a marked increase in MPO activity in the ulcer region in the control group, no significant increase was seen in the rebamipide group on days 100 and 140, showing that neutrophil infiltration was suppressed by rebamipide. Tanaka et al evaluated the impact of rebamipide on the barrier function of human corneal epithelial cells.[16] Rebamipide increased barrier function and suppressed TNF-α induced expression of IL-6 and 8. In primary human conjunctival epithelial cells Ueta et al observed that rebamipide suppressed the expression of CXCL10 and 11, RANTES, MCP-1 and IL-6, and eosinophil infiltration.[18]

These pharmacological actions require a rebamipide concentration of more than 1 to 100 μM based on in vitro studies.[15] Most orally ingested rebamipide is not absorbed from the digestive tract and the serum concentration is lower than 1 μM after oral intake of a regular dose.[4] To increase the local concentration of rebamipide in damaged tissue above this threshold it is given as a therapeutic agent in direct contact. It is used as an oral medicine for gastritis and gastric ulcers,[19] as eye drops for dry eyes[20] and as an enema for colitis, such as ulcerative colitis,[9] radiation proctitis[10] and ischemic colitis.[11] Because the anatomy of the bladder also makes local application of drugs possible, bladder inflammatory disease could be a candidate for rebamipide treatment.

A portion of rebamipide directly permeates the gastric mucosa and remains in the gastric wall after oral intake. Nakamura et al investigated the distribution of orally administered rebamipide in the stomach in an acetic acid induced gastric ulcer rat model.[21] Rebamipide was present in the submucosal layer, bound to infiltrated inflammatory cells. These findings were more pronounced in the gastritis group. Acrolein is transformed from CYP in the liver and continues to be excreted in urine for more than 1 hour.[22] We suggest that rebamipide instilled in the bladder penetrates the bladder wall, as occurs in the stomach, and continues to suppress bladder inflammation after excretion. The distribution of intravesically instilled rebamipide should be investigated in a future study.

In this series we used the composition of a vehicle that was clinically developed as eye drops. We diluted and dissolved this 2% suspension used as eye drops to 10 and 1 mM. Thus, we consider that the components used in this study should be safe enough for clinical application.

A study limitation is the inadequacy of the design. We administered CYP and rebamipide simultaneously, and noted that rebamipide prevented inflammation in the bladder. However, to our knowledge it is still unknown whether rebamipide cures preexisting inflammation, as demonstrated in a gastritis model. The study would have had greater clinical significance if the therapeutic effects of rebamipide had been identified after inflammation was established and not only preemptively. In addition, bladder inflammation up-regulates the expression of nociceptive receptors on nerve terminals and the production of neurotransmitters. Therefore, it is possible that rebamipide suppresses these reactions by suppressing inflammation. Further studies of these points are required to assess the possibility of using rebamipide as a new treatment option for bladder inflammatory disease.

CONCLUSIONS

Intravesical rebamipide relieved bladder overactivity in a CYP induced cystitis model by suppressing the inflammatory reaction in a dose dependent manner. This approach may be a new strategy for preventing chemically induced cystitis.

REFERENCES

1. Yamada S, Naito Y, Takagi T et al: Rebamipide ameliorates indomethacin-induced small intestinal injury in rats via the inhibition of matrix metalloproteinases activity. J Gastroenterol Hepatol 2012; **27:** 1816.
2. Hashimoto K, Oshima T, Tomita T et al: Oxidative stress induces gastric epithelial permeability through claudin-3. Biochem Biophys Res Commun 2008; **376:** 154.
3. Qi Z, Jie L, Haixia C et al: Effect of rebamipide on quality of peptic ulcer healing in rat. Dig Dis Sci 2009; **54:** 1876.
4. Akamatsu T, Nagaya T, Ichikawa S et al: Small bowel tissue concentration of rebamipide: study of two dosages in healthy subjects. J Clin Biochem Nutr 2010; **47:** 256.
5. Takagi T, Naito Y, Uchiyama K et al: Rebamipide promotes healing of colonic ulceration through enhanced epithelial restitution. World J Gastroenterol 2011; **17:** 3802.
6. Diao L, Mei Q, Xu JM et al: Rebamipide suppresses diclofenac-induced intestinal permeability via mitochondrial protection in mice. World J Gastroenterol 2012; **18:** 1059.
7. Gohil P, Thakkar H, Gohil U et al: Preliminary studies on the effect of rebamipide against the trypsin and egg-albumin induced experimental model of asthma. Acta Pharm 2011; **61:** 427.
8. Urashima H, Takeji Y, Okamoto T et al: Rebamipide increases mucin-like substance contents and periodic acid Schiff reagent-positive cells density in normal rabbits. J Ocul Pharmacol Ther 2012; **28:** 264.
9. Furuta R, Ando T, Watanabe O et al: Rebamipide enema therapy as a treatment for patients with active distal ulcerative colitis. J Gastroenterol Hepatol 2007; **22:** 261.
10. Kim TO, Song GA, Lee SM et al: Rebamipide enema therapy as a treatment for patients with chronic radiation proctitis: initial treatment or when other methods of conservative management have failed. Int J Colorectal Dis 2008; **23:** 629.
11. Matsumoto S, Tsuji K and Shirahama S: Rebamipide enema therapy for left-sided ischemic colitis patients accompanied by ulcers: open label study. World J Gastroenterol 2008; **14:** 4059.
12. Nasrin S, Masuda E, Kugaya H et al: Improvement by phytotherapeutic agent of detrusor overactivity, down-regulation of pharmacological receptors and urinary cytokines in rats with cyclophosphamide induced cystitis. J Urol 2013; **189:** 1123.
13. Zhang HP, Li CL, Lu P et al: The function of P2X3 receptor and NK1 receptor antagonists on cyclophosphamide-induced cystitis in rats. World J Urol 2013. Epub ahead of print.
14. Funahashi Y, Oguchi T, Goins WF et al: Herpes simplex virus vector mediated gene therapy of tumor necrosis factor-alpha blockade for bladder overactivity and nociception in rats. J Urol 2013; **189:** 366.
15. Banan A, Fitzpatrick L, Zhang Y et al: OPC-compounds prevent oxidant-induced carbonylation

and depolymerization of the F-actin cytoskeleton and intestinal barrier hyperpermeability. Free Radic Biol Med 2001; **30:** 287.

16. Tanaka H, Fukuda K, Ishida W et al: Rebamipide increases barrier function and attenuates TNFalpha-induced barrier disruption and cytokine expression in human corneal epithelial cells. Br J Ophthalmol 2013; **97:** 912.

17. Sakurai K, Osaka T and Yamasaki K: Rebamipide reduces recurrence of experimental gastric ulcers: role of free radicals and neutrophils. Dig Dis Sci, suppl., 2005; **50:** S90.

18. Ueta M, Sotozono C, Yokoi N et al: Rebamipide suppresses Polyl:C-stimulated cytokine production in human conjunctival epithelial cells. J Ocul Pharmacol Ther 2013; **29:** 688.

19. Shin WG, Kim SJ, Choi MH et al: Can rebamipide and proton pump inhibitor combination therapy promote the healing of endoscopic submucosal dissection-induced ulcers? A randomized, prospective, multicenter study. Gastrointest Endosc 2012; **75:** 739.

20. Kinoshita S, Awamura S, Oshiden K et al: Rebamipide (OPC-12759) in the treatment of dry eye: a randomized, double-masked, multicenter, placebo-controlled phase II study. Ophthalmology 2012; **119:** 2471.

21. Nakamura M, Akiba Y, Matsui H et al: Rebamipide binds to iNOS-positive cells in acetic acid-treated but not in ethanol-treated rat gastric mucosa. Aliment Pharmacol Ther, suppl., 2004; **18:** 76.

22. Wagner T, Heydrich D, Jork T et al: Comparative study on human pharmacokinetics of activated ifosfamide and cyclophosphamide by a modified fluorometric test. J Cancer Res Clin Oncol 1981; **100:** 95.

Am J Physiol Renal Physiol 305: F1796–F1803, 2013.
First published October 9, 2013; doi:10.1152/ajprenal.00151.2013.

A 5-hydroxytryptamine receptor antagonist, sarpogrelate, reduces renal tubulointerstitial fibrosis by suppressing PAI-1

Yoshifumi Hamasaki,[1,4] Kent Doi,[1,2] Rui Maeda-Mamiya,[1] Emi Ogasawara,[1] Daisuke Katagiri,[1] Tamami Tanaka,[1] Tokunori Yamamoto,[5] Takeshi Sugaya,[6] Masaomi Nangaku,[1] and Eisei Noiri[1,3,7]

[1]Department of Nephrology and Endocrinology, The University of Tokyo, Tokyo, Japan; [2]Department of Emergency and Critical Care Medicine, The University of Tokyo, Tokyo, Japan; [3]Department of Apheresis and Dialysis, The University of Tokyo, Tokyo, Japan; [4]22nd Century Medical and Research Center, University Hospital, The University of Tokyo, Tokyo, Japan; [5]Department of Urology, Nagoya University, Nagoya, Japan; [6]CMIC Company, Limited, Tokyo, Japan; and [7]Japan Science and Technology Agency/Japan International Cooperation Agency (JST/JICA), Science and Technology Research Partnership for Sustainable Development (SATREPS), Tokyo, Japan

Submitted 13 March 2013; accepted in final form 2 October 2013

Hamasaki Y, Doi K, Maeda-Mamiya R, Ogasawara E, Katagiri D, Tanaka T, Yamamoto T, Sugaya T, Nangaku M, Noiri E. A 5-hydroxytryptamine receptor antagonist, sarpogrelate, reduces renal tubulointerstitial fibrosis by suppressing PAI-1. *Am J Physiol Renal Physiol* 305: F1796–F1803, 2013. First published October 9, 2013; doi:10.1152/ajprenal.00151.2013.—A selective 5-hydroxytryptamine (5-HT) 2A receptor antagonist sarpogrelate (SG) blocks serotonin-induced platelet aggregation. It has been used clinically for the treatment of peripheral arterial disease. SG might be able to improve chronic ischemia, which contributes to renal fibrosis progression by maintaining renal microcirculation. This study investigated whether SG suppresses renal fibrosis. C57BL/6 mice fed a 0.2% adenine-containing diet for 6 wk developed severe tubulointerstitial fibrosis with kidney dysfunction. Subsequent SG treatment (30 $mg \cdot kg^{-1} \cdot day^{-1}$) for 4 wk improved these changes significantly by increasing peritubular blood flow in the fibrotic area, as evaluated by intravital microscopy and decreasing fibrin deposition. Urinary L-type fatty acid-binding protein, up-regulated by renal hypoxia, was also reduced by SG. Additionally, results showed that mRNA expression of plasminogen activator inhibitor-1 (PAI-1), which is known to promote fibrosis by mediating and enhancing transforming growth factor (TGF)-β1 signaling, was suppressed by SG treatment in the kidney. In vitro experiments using cultured murine proximal tubular epithelial (mProx) cells revealed that incubation with TGF-β1 and 5-HT increased PAI-1 mRNA expression; SG significantly reduced it. In conclusion, SG reduces renal fibrosis not only by the antithrombotic effect of maintaining peritubular blood flow but also by suppressing PAI-1 expression in renal tubular cells.

L-FABP; PAI-1; peritubular blood flow; sarpogrelate; tubulointerstitial fibrosis

THE INCIDENCE AND PREVALENCE of chronic kidney disease (CKD) continue to increase, entailing poor outcomes and high costs (3, 49). CKD is well known to contribute strongly to cardiovascular disease and high mortality (7, 19, 33, 42). Although CKD progresses slowly, it eventually evolves to end-stage renal disease, which necessitates renal replacement therapy such as dialysis or kidney transplantation (37). The best predictive factor for progression of CKD to end-stage renal disease is not the etiology of glomerular injury but the degree of tubulointerstitial damage such as fibrosis and inflammatory cell infiltration (26, 31, 37, 39). Tubulointerstitial fibrosis is a common pathological change occurring in association with chronic kidney damage (38).

5-Hydroxytryptamine (5-HT), synthesized from L-tryptophan and stored in platelets, is subsequently secreted, promoting not only platelet aggregation but also proliferation of vascular smooth muscle cells, leading to vascular occlusion at the site of vascular injury (51). The 5-HT2A receptor, one of seven 5-HT receptor subfamilies, mediates the effect of 5-HT on platelet aggregation and vasoconstriction. It is known that the system for 5-HT synthesis is present in the kidney and that 5-HT signaling through the 5-HT2A receptor accelerates the expression of transforming growth factor (TGF)-β1 in cultured cells derived from the kidney (9, 17, 44, 53). Sarpogrelate (SG), a selective antagonist of the 5-HT2A receptor, is widely used for the treatment of peripheral arterial disease and cardiovascular disease because of its vasodilation and antiplatelet effects (12, 40). SG in combination with antidiabetic agents increases plasma levels of adiponectin, an adipokine, in diabetic patients with peripheral arterial disease (54). Although renoprotective effects of SG in animal models of glomerulonephritis and diabetic nephropathy have been described in several reports (6, 16, 17, 22), the protective effects of SG on renal fibrosis or renal tubular cells remain unclear.

Plasminogen activator inhibitor-1 (PAI-1) is a 50-kDa single-chain glycoprotein with serine proteinase inhibitor activity. PAI-1 inhibits fibrinolysis and plays a role in the pathogenesis of thrombosis in diseases such as coronary artery disease (23). During the past decade, many studies using various animal models have demonstrated that PAI-1 is an important downstream effector of TGF-β1 and that PAI-1 promotes tissue fibrosis (5, 10, 24). PAI-1, which serves a crucial role in promoting renal fibrosis, is anticipated as a therapeutic target to prevent CKD (5). Some reports have described a link between 5-HT signaling mediated by the 5-HT2A receptor and PAI-1. PAI-1 expression in vascular endothelial cells, which is induced by 5-HT stimulation, is improved by treatment with SG (18). Furthermore, PAI-1 expression is reduced by the administration of SG or knockdown of the 5-H2A receptor in adipocytes (50). These findings indicate the possibility that antagonism of 5-HT2A receptors decreases PAI-1 expression. However, it remains unknown whether SG improves renal fibrosis by reducing PAI-1 expression in the kidney.

This study examined the protective effect of SG on a mouse renal tubulointerstitial fibrosis model, which is induced by feeding mice an adenine-containing diet (Ad) for several weeks

Address for reprint requests and other correspondence: K. Doi, Dept. of Emergency and Critical Care Medicine, The Univ. of Tokyo, 7-3-1 Hongo, Bunkyo, Tokyo 113-8655, Japan (e-mail: kdoi-tky@umin.ac.jp).

(47). We further examined peritubular blood flow and urinary L-type fatty acid-binding protein (L-FABP) excretion to evaluate renal ischemia and hypoxia, as reported previously (15, 48, 56). We also performed in vitro analysis with murine proximal tubular epithelial (mProx) cells to investigate whether PAI-1 expression in proximal tubular epithelial cells is upregulated by 5-HT stimulation and improved by SG treatment.

MATERIALS AND METHODS

Animal experiments. Eight-week-old male wild-type C57BL/6 mice were used in this experiment. Male heterozygous hL-FABP transgenic (Tg) mice (C57BL/6 background), weighing 25–35 g, were also used to evaluate urinary hL-FABP. The engineering of hL-FABP Tg mice was described previously (15, 56). All experiments were conducted in accordance with the National Institutes of Health *Guide for the Care and Use of Laboratory Animals* (U.S. Department of Health and Human Services, Public Health Service, National Institutes of Health, NIH Publication No. 86-23, 1985) and were approved by The University of Tokyo Institutional Review Board.

Both the SG-treated group (Ad+SG group) and the untreated group (Ad group) were fed a 0.2% wt/wt adenine-containing diet (Oriental Yeast, Tokyo, Japan) for 6 wk. The Ad+SG group was administered SG (generously provided by Mitsubishi Tanabe Pharma, Osaka, Japan) dissolved in distilled water for 4 wk from 2 wk after starting the adenine-containing diet, similarly to a process used in a previous study demonstrating the effect of a drug against tubulointerstitial fibrosis (11). Based on doses of SG administrated to various animal models in previous studies (13, 34), we chose the dosage of SG for the present study to be equal to those used in previous studies (30 $mg \cdot kg^{-1} \cdot day^{-1}$). The dosage of SG was based on evidence that SG suppresses platelet aggregation and formation of platelet-rich thrombus by blockade of 5-HT2A receptors in rodents (12). To evaluate the dose-response effect of SG to suppress chronic kidney injury induced by an adenine-containing diet, three different dosages (3, 30, and 300 $mg \cdot kg^{-1} \cdot day^{-1}$) were evaluated. The SG solution concentration was adjusted to give mice 3, 30, and 300 mg/kg SG daily based on the amount of drinking water consumed. The Ad group was given distilled water only. The normal-diet group (N group) was fed a normal diet and given water for 6 wk. The normal diet was purchased from Oriental Yeast. Its components were identical to those of the adenine-containing diet except for adenine. Body weights of mice were measured and blood samples were collected every 2 wk after the start of the adenine-containing diet.

Blood chemistry. Blood urea nitrogen (BUN) was measured using the urease-indophenol method (Urea N B test; Wako Pure Chemical Industries, Osaka, Japan). Plasma creatinine (Cre) measurements using HPLC were conducted as described previously (60).

Pathological analysis. Kidneys were collected at 6 wk after the start of the adenine-containing diet, fixed in 10% buffered formalin, and embedded in paraffin. Sections (2 μm thick) were cut and used for Masson's trichrome (MT) and immunohistochemistry. After antigen retrieval with 100 μM proteinase K for 30 min, an anti-human fibrin-fibrinogen antibody (Dako Denmark, Glostrup, Denmark) was used for fibrin immunohistochemical staining, as previously described (57). After microwave boiling of tissue for 10 min in 10 mM sodium citrate buffer (pH 6.0), immunostaining for PAI-1 and type IV collagen was conducted respectively using a rabbit polyclonal anti-PAI-1 antibody (H-135; Santa Cruz Biotechnology, Santa Cruz, CA) and type IV collagen antibody (Abcam, Cambridge, UK). Immunohistochemistry for F4/80 and α-smooth muscle actin (α-SMA) was performed as described previously (47). The interstitial fibrotic area, fibrinogen-positive area, F4/80-positive macrophages, α-SMA-positive area, and type IV collagen-positive area were evaluated using a computer-aided evaluation program (AIS; Imaging Research, St. Catharines, ON) as described previously (47).

Measurement of peritubular blood flow. Peritubular capillary images of mice were obtained using an intravital video charge-coupled device (CCD) 4 wk after the start of the adenine-containing diet. Renal capillary blood flow was visualized and measured according to a previously reported method (55, 56).

Measurement of urinary human L-FABP by ELISA. Male human L-FABP transgenic mice were kept in glass-shielded metabolic cages for 4 wk after starting the adenine-containing diet for 24 h to collect urine. To evaluate proximal tubular injury, urinary human L-FABP was measured using a sandwich ELISA kit (CMIC, Tokyo, Japan) as described previously (32, 56). Urinary human L-FABP levels are expressed as the ratio to the urinary creatinine concentration measured using a commercial kit (Nescoat VLII CRE, Alfresa Pharma, Osaka, Japan). Measurements were performed in duplicate.

Cell culture. The stable C57BL/6 mice proximal tubular epithelial cell line mProx was obtained as described previously (56) and cultured in DMEM (containing 10% FBS, 100 U/ml penicillin G, and 100 μg/ml streptomycin; GIBCO, Carlsbad, CA) in a humidified atmosphere containing 5% CO_2 at 37°C. The mProx cells were seeded on 12-well culture plates in complete medium containing 10% FBS. After mProx cells were grown to 80% confluence, the cells were kept in medium containing 0.5% FBS for 24 h. Then, they were placed into the serum-free medium containing 5 ng/ml recombinant human TGF-β1 (Sigma-Aldrich, St. Louis, MO) for 24 h. Thereafter, mProx cells were incubated with serum-free medium with 10 μM 5-HT and 10 μM SG for 3 h. Based on the previous study showing dose-dependent effects of 5-HT and cytotoxicity of SG by the concentration of more than 10 μM, we decided on the concentration of 5-HT and SG in this study (6). PAI-1 mRNA expression in mProx cells was increased significantly after 3 h incubation with 5-HT following TGF-β1 stimulation when it was evaluated in the different time courses (3, 6, 12 h) in our preliminary study. Therefore, we decided to incubate mProx cells with 5-HT and SG for 3 h. Cells were washed with PBS three times and lysed using TRIzol Reagent (Invitrogen, Carlsbad, CA) to extract total RNA.

Quantitative PCR analysis of PAI-1, monocyte chemoattractant protein-1, and 5-HT2A receptor expression. Total RNA isolated from the harvested kidneys or mProx cells were reverse transcribed to cDNA using recombinant Moloney leukemia virus reverse transcriptase and random hexamers (High Capacity cDNA Reverse Transcription Kit; Applied Biosystems, Carlsbad, CA). Transcripts encoding PAI-1 and monocyte chemoattractant protein-1 (MCP-1) were measured using TaqMan real-time quantitative PCR with the Prism 7000 sequence detection system (Applied Biosystems, Foster City, CA) and TaqMan Universal PCR master mix (Applied Biosystems) as described previously (47). The TaqMan probes and primers for PAI-1 (assay identification number Mm01310498_m1), and MCP-1 (assay identification number Mm00441242_m1) were assay-on-demand gene expression products (Applied Biosystems). To normalize for variance in loaded cDNA, 18S ribosomal RNA (18S rRNA) was amplified in a separate tube using TaqMan-based quantitative PCR. Probe primers for 18S rRNA were obtained from Applied Biosystems. Standard curves were prepared for each gene and the 18S rRNA in each experiment to normalize the relative expression of the genes of interest to the 18S rRNA control.

To investigate whether the 5-HT2A receptor is expressed in mProx cells derived from C57BL/6 mice and kidneys, transcripts encoding the 5-HT2A receptor and GAPDH were amplified by PCR. Then, PCR products were electrophoresed in 2% agarose 1× TAE gel. The sequences of primers are as follows: murine 5-HT2A receptor (forward: 5′-CCAGCGGTCCATCCACAGAG-3′; reverse: 5′-ACCACATTACAACAAACAGAAAGAACAC-3′), murine GAPDH (forward: 5′-ACCACAGTCCATGCCATCAC-3′; reverse: 5′-TCCACCACCCTGTTGCTGTA-3′). PCR products were visualized using GelGreen (Biotium, Hayward, CA) and a CCD camera system (LAS-4000 mini; Fuji Photo Film, Tokyo, Japan).

Statistical analysis. Results are expressed as means ± SE. Differences among experimental groups were determined using one-way ANOVA with post hoc analysis (Tukey-Kramer test) for multiple comparison. Differences of $P < 0.05$ were considered significant.

RESULTS

Effects of SG on renal function and histopathological changes in adenine-induced mouse tubulointerstitial injury model. To evaluate dose-response effects of SG for protection of the kidney in an adenine-induced mouse tubulointerstitial injury model, mice were treated with three different doses of SG. Both BUN and Cre concentrations in the 30 mg·kg^{-1}·day^{-1} SG treatment group [middle-dose (M) group] were significantly lower than in the no treatment group (Ad group), although those in the 3 mg·kg^{-1}·day^{-1} SG treatment [low-dose (L)] group and the 300 mg·kg^{-1}·day^{-1} SG treatment [high-dose (H)] group were not (Fig. 1, *A* and *B*). Fibrin deposition in the kidneys of the M group was significantly reduced compared with that in the Ad group. However, those in the L and H groups were not (Fig. 1, *C* and *D*). According to these results, we decided to pursue further experiments with the dose of 30 mg·kg^{-1}·day^{-1}.

The body weight of mice in the adenine diet group was significantly lower than the normal diet group from 2 wk after starting the adenine-containing diet (Fig. 2*A*). BUN levels in the adenine diet group were significantly higher than those of the normal-diet (N) group 2 wk after the start of the adenine diet [N group, 28.2 ± 0.5 mg/dl (n = 5); adenine diet group, 62.1 ± 3.7 mg/dl (n = 20)]. Mice in the adenine diet group were divided equally into two groups at 2 wk: the vehicle only (Ad) group and the SG treatment (Ad+SG) groups. The levels of BUN and Cre in the Ad+SG group (n = 10) were significantly lower than the Ad group (n = 10) at 4 and 6 wk (Fig. 2, *B* and *C*), although SG had no effect on the body weight of mice in these two groups (Fig. 2*A*). Pathological evaluation showed remarkable interstitial fibrosis, irregular renal tubular dilatation, and deposition of fibrin in the kidney of mice fed the adenine-containing diet at 6 wk (Fig. 3*A*). Quantitative analyses of the fibrotic area and fibrin-positive area revealed that SG improved these histopathological changes (Fig. 3, *B* and *C*). PAI-1 expression in tubular epithelial cells was increased in the adenine diet group and was reduced significantly by SG treatment (Fig. 3, *A* and *D*). F4/80-positive inflammatory cell (macrophage) infiltration in the interstitium was increased by adenine administration and reduced by SG treatment (Fig. 3, *A* and *E*). The levels of expression of both α-SMA and type IV collagen were significantly increased in the kidneys of mice fed the adenine-containing diet and were improved by SG treatment (Fig. 3, *A*, *F*, and *G*).

Effects of SG on PAI-1, MCP-1, and TGF-β1 expression in the kidney. The mRNA expressions of PAI-1, MCP-1, and TGF-β1 in the kidney were increased significantly by adenine administration. PAI-1 expression was reduced significantly by SG treatment (Fig. 4*A*). The expression of MCP-1 was not changed significantly by SG treatment (Fig. 4*B*), whereas TGF-β1 tended to be decreased by SG with no statistical significance (Fig. 4*C*).

Evaluation of peritubular blood flow in the kidney. We evaluated peritubular blood flow in an adenine-induced renal injury model using intravital video CCD images at 4 wk. In the Ad group, peritubular blood flow was significantly decreased compared with that of the N group. Animals treated with SG showed significantly higher blood flow than did the untreated animals (Fig. 5*A*).

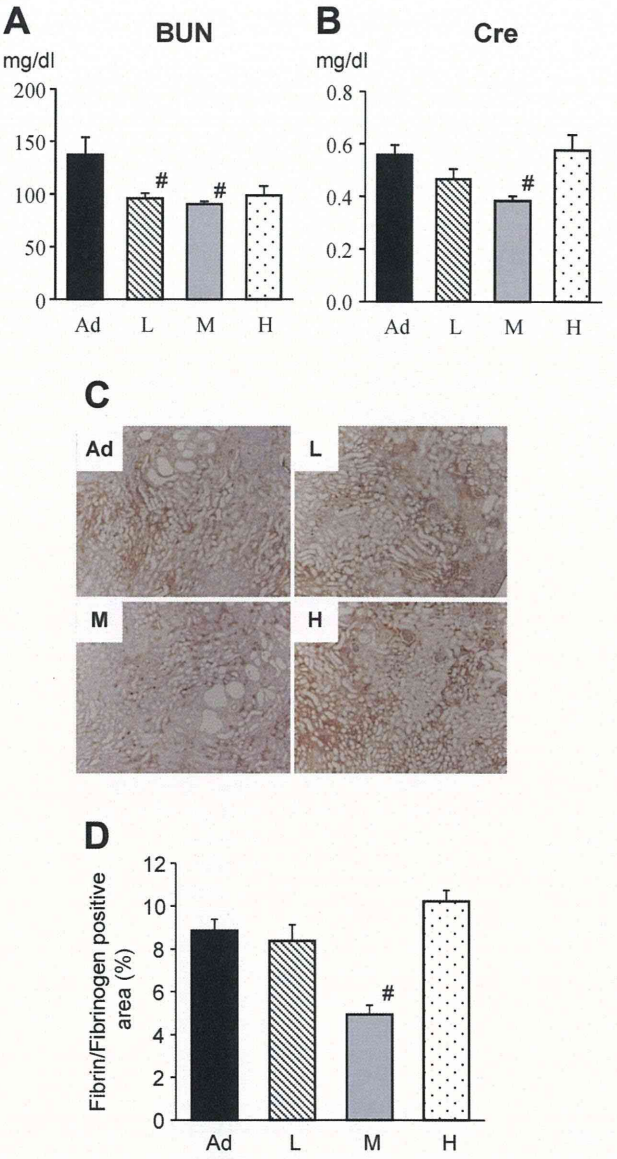

Fig. 1. Dose-response of sarpogrelate on mouse adenine-induced tubulointerstitial injury model. Levels of blood urea nitrogen (BUN) and plasma creatinine (Cre) of mice groups treated with different doses of SG were measured at 6 wk (*A* and *B*). Renal fibrin deposition was evaluated using immunohistochemistry, and the fibrin-positive area was quantified (*C* and *D*). Ad, adenine diet; L, adenine diet and 3 mg·kg^{-1}·day^{-1} sarpogrelate treatment; M, adenine diet and 30 mg·kg^{-1}·day^{-1} treatment; H, adenine diet and 300 mg·kg^{-1}·day^{-1} sarpogrelate treatment. Values are means ± SE; n = 15 in the Ad and M group each, and n = 11 in the L and H group each. #$P < 0.05$ vs. Ad group.

Effects of SG on urinary excretion of L-FABP. Reportedly, urinary L-FABP levels in the adenine-induced mouse tubulointerstitial injury model reflect the degree of fibrosis (47). Urinary secretion of L-FABP was apparently induced by hypoxia (4). In the current study, urinary L-FABP level was increased in the Ad group at 4 wk after the beginning of the adenine-containing diet. SG reduced urinary L-FABP levels significantly (Fig. 5*B*).

Expression of 5-HT receptors and PAI-1 in renal proximal tubular epithelial cells. We conducted in vitro experiments using mProx cells. In mProx cells, expression of the 5-HT2A

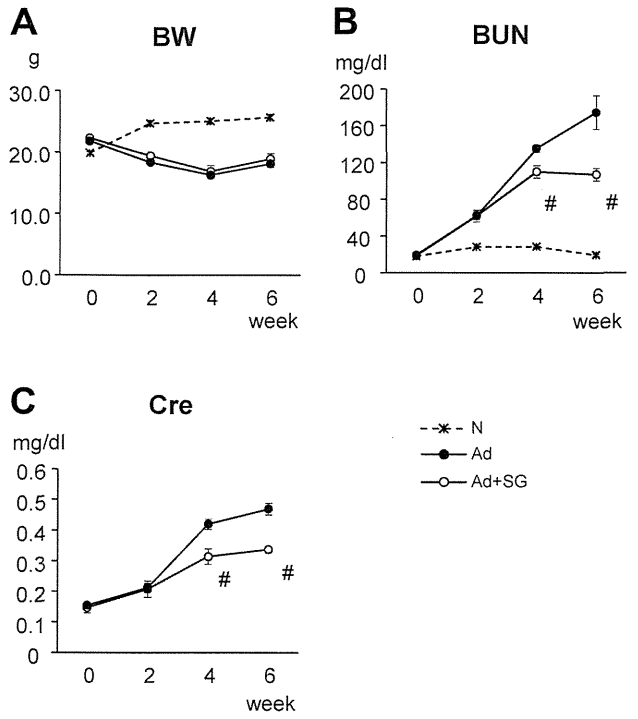

Fig. 2. Effect of sarpogrelate on mouse adenine-induced tubulointerstitial injury model. Course of body weight (BW), blood urea nitrogen (BUN), and plasma creatinine (Cre) levels are presented. BW, BUN, and Cre were measured at 0, 2, 4, and 6 wk (*A–C*). N, normal diet; Ad, adenine diet; Ad+SG, adenine diet and sarpogrelate treatment. Values are means ± SE; $n = 5$ in the N group and $n = 10$ in the Ad group and Ad+SG group each. #$P < 0.05$ vs. Ad group at the same time point.

receptor, for which SG has high affinity, was confirmed by RT-PCR as in the mouse kidney (Fig. 6*A*). An in vitro model of tubular injury was induced by incubating mProx cells with TGF-β1 (5 ng/ml) and 5-HT (10 μM). On quantitative real-time PCR, PAI-1 expression was increased significantly by TGF-β1 and was increased further by addition of 5-HT (Fig. 6*B*). In our preliminary experiments, mRNA expression of PAI-1 was not increased significantly in the mProx cells stimulated by 5-HT without TGF-β1 compared with the control cells. SG treatment significantly reduced PAI-1 expression in mProx cells incubated with TGF-β1 and 5-HT (Fig. 6*B*).

DISCUSSION

A selective 5-HT2A receptor antagonist, SG, is used clinically for prevention of platelet aggregation and subsequent thrombosis formation. This study demonstrated that SG ameliorated renal dysfunction and pathological changes in fibrosis in a mouse tubulointerstitial injury model. SG reduced fibrin deposition and maintained renal microcirculation. Moreover, SG significantly suppressed the increase in PAI-1 expression levels in the fibrotic kidney. We further demonstrated that PAI-1 expression was upregulated synergistically by TGF-β1 and 5-HT in mProx cells and that it was reduced significantly by SG treatment. Results show for the first time that suppression of PAI-1 by SG can ameliorate the progression of renal fibrosis.

In this study, we investigated renoprotective effects of SG using an adenine-induced tubulointerstitial fibrosis model. The adenine-induced chronic renal failure, originally described in rats, has been regarded as a useful animal model of CKD because it resembles human uremic features such as renal dysfunction, severe anemia, and secondary hyperparathyroidism (1, 45, 59). An adenine-induced CKD model in C57BL/6 mice was also developed, and several experimental reports using this model using mice have been published recently (41, 46, 47). Renal fibrosis is another characteristic of this model. Mice fed with an adenine-containing diet show renal fibrosis as severe as that in mice with unilateral ureteral obstruction (UUO) (11, 29). The mechanism of renal injury is regarded as follows. Adenine in the chow is oxidized to 2,8-dihydroxyadenine by xanthine dehydrogenase after intestinal absorption. Then, 2,8-dihydroxyadenine will be precipitated in renal tubules because of its low solubility. Deposition of 2,8-dihydroxyadenine crystals degenerates renal tubular epithelial cells and causes inflammatory injury with subsequent fibrotic changes.

In CKD, the uptake of synthesized 5-HT into platelets is decreased and the plasma concentration of 5-HT is increased (27), which suggests that increased 5-HT concentration in the systemic circulation might contribute to the progression of CKD. Reportedly, SG can improve glomerular injury through several different mechanisms such as reducing glomerular platelet activation in a rat diabetic nephropathy model (22), or inhibiting 5-HT-induced type IV collagen secretion and suppressing mitogenic signaling in cultured mesangial cells (6, 17). Reportedly, 5-HT signaling through the 5-HT2A receptor accelerates the expression of TGF-β1 via the PKC-MEK-ERK pathway in mesangial cells (9, 17). Are mesangial cells in glomeruli the only target of the 5-HT-related pathway? In this study, we used a mouse tubulointerstitial injury model by administering adenine, in which no obvious glomerular lesion such as sclerosis or mesangial expansion was observed (47). In this study, although fibrin deposition and PAI-1 expression were observed in some glomeruli in addition to tubulointerstitium of the adenine diet group, no glomerular change induced by chronic glomerular damage such as global sclerosis was observed. Tubulointerstitial fibrosis induced by chronic tubulointerstitial injury was diffuse and severe. Renal injury induced by adenine is thought to derive from renal tubular occlusion with 2,8-dihydroxyadenine crystals (59). Therefore, it is reasonable to infer that glomerular change follows tubulointerstitial injury in this model. To improve tubulointerstitial injury by SG treatment in this animal model, some mechanism of action other than glomerular protection by SG is suggested.

PAI-1 is regarded as playing a critical regulatory role in fibrosis. Although elevated PAI-1 promotes fibrosis, decreased PAI-1 reduces it, but the mechanism of these effects remains elusive (25). Reportedly, tubulointerstitial fibrosis was worsened by PAI-1 overexpression and was ameliorated by knocking down of PAI-1 in an ureteral obstruction-induced renal fibrosis model (28, 35). PAI-1 expression is induced by TGF-β1 through upregulation of reactive oxygen species (ROS), but TGF-β1 expression is accelerated by PAI-1 (5, 10). Therefore, PAI-1 will not only act as an effector of TGF-β1 but will also constitute a positive feedback loop together with TGF-β1 in renal fibrosis progression (43). PAI-1 expression was increased not only by TGF-β1 but also by 5-HT stimulation in endothelial cells or adipocytes (18, 50). In this study, the levels of PAI-1 and TGF-β1 expression in the kidney were increased by feeding mice an adenine-containing diet. In vitro analysis showed synergistically increased PAI-1 expression by 5-HT and TGF-β1 in mProx cells.

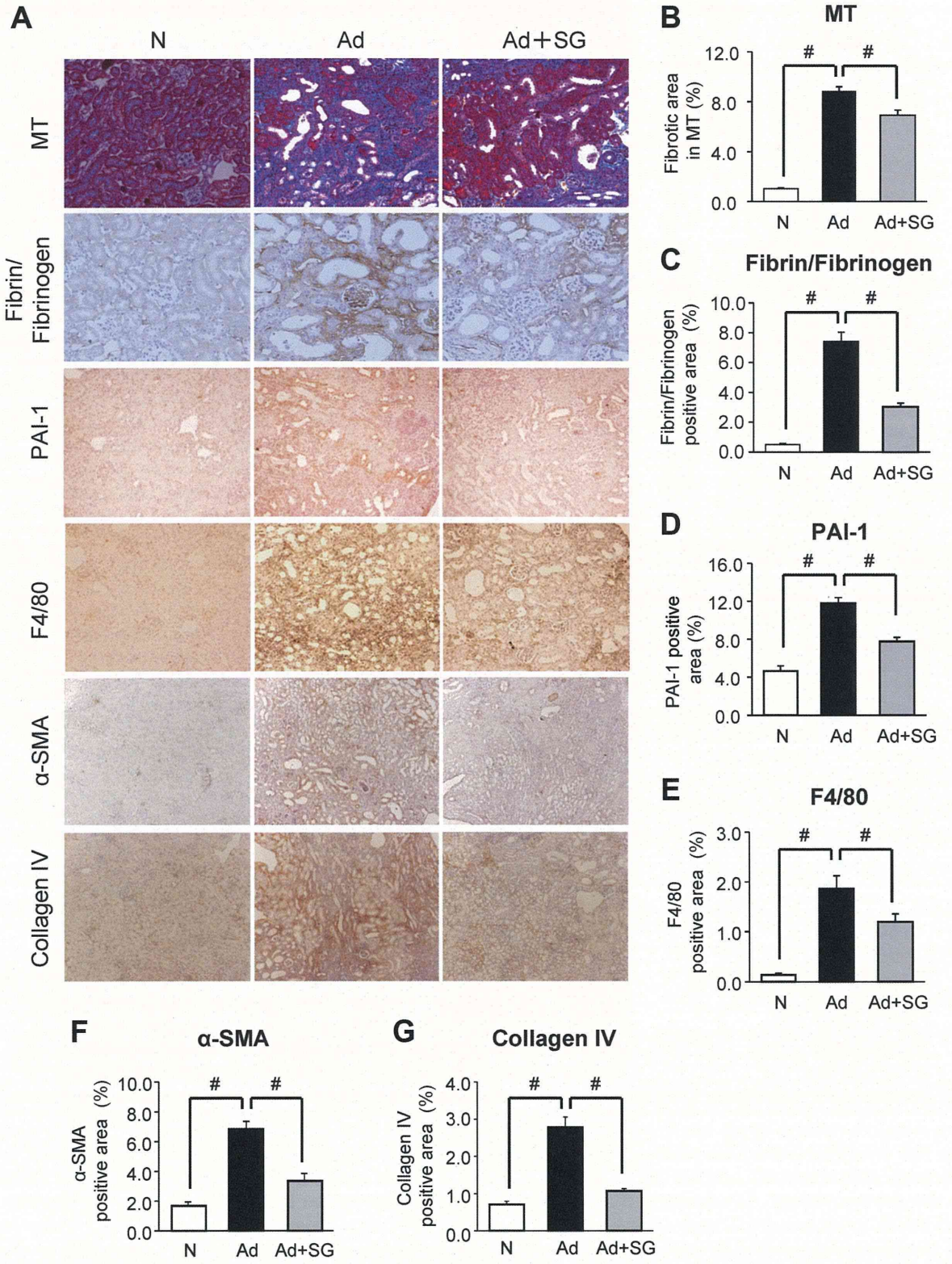

Fig. 3. Renal pathological findings in mouse adenine-induced tubulointerstitial injury model at 6 wk. Renal histological changes evaluated using Masson's trichrome (MT) staining and immunohistochemistry are shown (*A*). Original magnification: ×200. Fibrotic area in MT stain (*B*), positive staining area of fibrin (*C*), plasminogen activator inhibitor-1 (PAI-1; *D*), F4/80 (*E*), α-smooth muscle actin (SMA; *F*), and type IV collagen (*G*) were quantified. N, normal diet; Ad, adenine diet; Ad+SG, adenine diet and sarpogrelate treatment. Values are means ± SE; $n = 5$ in the N group and $n = 10$ in the Ad group and Ad+SG group each. #$P < 0.05$.

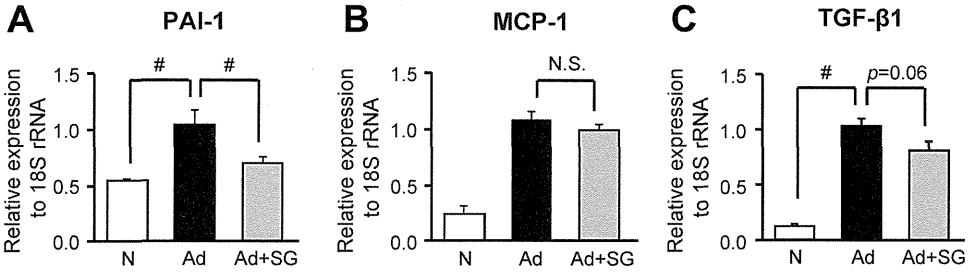

Fig. 4. mRNA expressions of PAI-1, monocyte chemoattractant protein-1 (MCP-1), and transforming growth factor (TGF)-β1 in mouse adenine-induced tubulointerstitial injury model. Expressions of PAI-1 (*A*), MCP-1 (*B*), and TGF-β1 (*C*) were evaluated using quantitative real-time PCR. N, normal diet; Ad, adenine diet; Ad+SG, adenine diet and sarpogrelate treatment. Values are means ± SE; $n = 5$ in the N group and $n = 10$ in the Ad group and Ad+SG group each. #$P < 0.05$.

A selective 5-HT2A receptor antagonist, SG, reduced PAI-1 expression both in vivo and in vitro. Additionally, we confirmed 5-HT2A receptor expression in mProx cells, as in the murine kidney (Fig. 6*A*) (36, 53). These observations indicated that PAI-1 expression triggered by TGF-β1 was accelerated by 5-HT via the 5-HT2A receptor.

We first demonstrated that SG ameliorated adenine-induced tubulointerstitial fibrosis in mice and that it significantly reduced the renal expression of PAI-1, which is known as a key molecule in renal fibrosis progression. Renal PAI-1 expression has been shown to be increased not only in chronic renal injury animal models such as UUO, 5/6 nephrectomy, and glomerulonephritis but also in human CKD patients (5, 8, 28). PAI-1 accelerates chronic kidney injury in various animal models. Therefore, it is possible that suppression of PAI-1 by SG treatment at least partly improves renal fibrosis in other animal models as well as it does in the adenine-induced renal fibrosis model. Recently, SG treatment was reported to improve liver fibrosis accompanied by a reduction in TGF-β and α-SMA; both were common molecules for which expressions were increased in renal fibrosis progression (20). Further evaluation must be done to confirm the renal-protective effect of SG in different animal models.

This study showed that peritubular blood flow in a fibrotic kidney was reduced significantly compared with that in a normal kidney. A relationship between microcirculation in the kidney and renal fibrosis has been suggested. Reportedly, renal microcirculation is reduced before progression of renal fibrosis

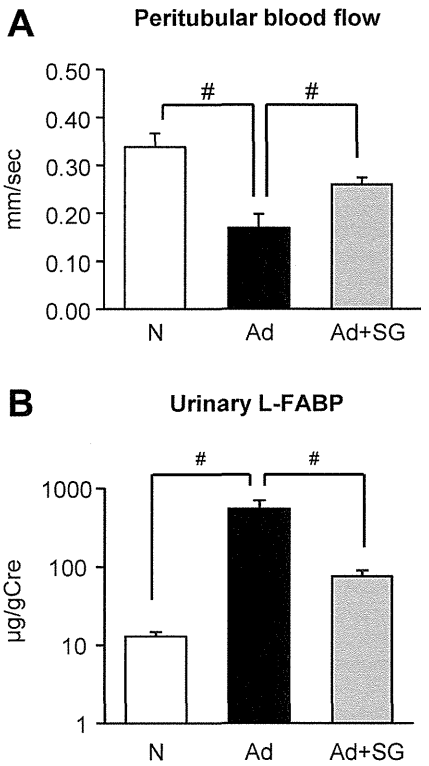

Fig. 5. Peritubular blood flow and urinary L-type fatty acid-binding protein (L-FABP) in mouse adenine-induced tubulointerstitial injury model. Peritubular blood flow was measured in the kidney of mice by intravital charge-coupled device (CCD) videoscopy (*A*). Urinary L-FABP was measured using 24-h collected urine at 4 wk: N, normal diet; Ad, adenine diet; Ad+SG, adenine diet and sarpogrelate treatment. Values are means ± SE; $n = 5$ in each group. #$P < 0.05$.

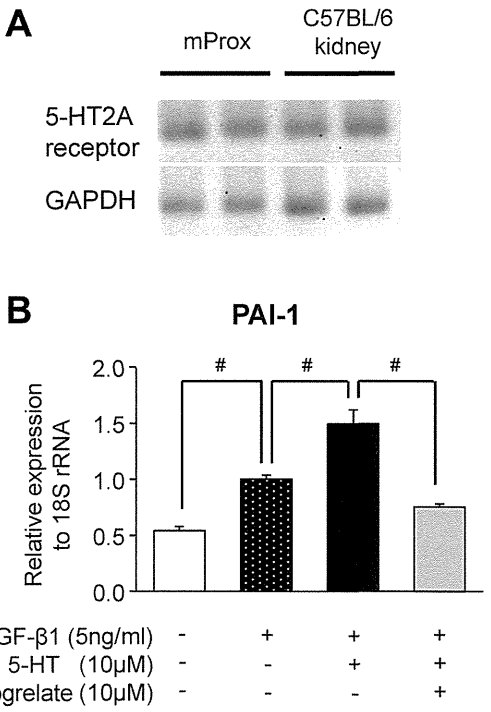

Fig. 6. Expressions of mRNA of 5-hydroxytryptamine (5-HT) 2A receptor and PAI-1 in mProx cells. Expression of 5-HT2A receptor in mProx cells and mouse kidney was evaluated by RT-PCR (*A*). PAI-1 expression in mProx cells was induced synergistically by 5-HT and TGF-β1 (*B*, black bar), and sarpogrelate suppressed PAI-1 expression (*B*, gray bar). Values are means ± SE; $n = 2$ (*A*) and $n = 8$–12 obtained from more than 3 independently conducted experiments in each group (*B*). #$P < 0.05$.

(2), and that protection of endothelial cells increases renal cortical blood flow and reduces renal fibrosis in UUO (21). Reportedly, tubulointerstitial hypoxia, derived from impaired blood flow in the kidney, might induce tubulointerstitial fibrosis and reduction of peritubular capillaries; the fibrosis, in turn, will impair the tubulointerstitial oxygen supply (26, 30). Therefore, reduced renal blood flow and tubulointerstitial fibrosis constitute a vicious cycle that accelerates renal injury. Although the 5-HT receptor antagonist ritanserin reportedly improved impairment of renal blood flow autoregulation by cyclosporine (52), no report in the relevant literature has described that SG, a selective 5-HT2A receptor antagonist, improves peritubular blood flow and renal fibrosis. SG might preserve blood flow directly by inhibiting aggregation of the platelets which causes thrombosis. Actually, results from our study showed that fibrin deposition in the kidney was reduced significantly by SG. SG apparently suppresses the vicious cycle between renal blood flow and renal fibrosis progression by ameliorating renal fibrosis via reducing TGF-β1 or PAI-1 expression in the kidney. Therefore, SG treatment might preserve microcirculation in the kidney by maintaining the normal structure of the peritubular capillary network.

Increased urinary L-FABP level showed significant correlation with decreased peritubular capillary blood flow and progression of tubulointerstitial fibrosis in human and animal models (47, 48, 56). Of note, urinary L-FABP levels in CKD patients were correlated to the progression of CKD and the degree of proteinuria (14). The promoter of the L-FABP gene contains the hypoxia-responding element. Therefore, hypoxic injury to renal tubular cells can be detected by measurement of urinary L-FABP (32, 56, 58). Moreover, a recent study demonstrated that urinary secretion of L-FABP is induced by renal hypoxia (4). In this study, urinary L-FABP concentration was increased in the Ad group and was reduced significantly by SG treatment accompanied by improvement of peritubular blood flow and tubulointerstitial fibrosis. Chronic hypoxia caused by decreased peritubular capillary blood flow attributable to tubulointerstitial damage might upregulate the expression of L-FABP.

In conclusion, SG prevented the progression of renal fibrosis by multiple pathways in a mouse tubulointerstitial injury model. Among those pathways, suppressing PAI-1 expression by SG was further confirmed by in vitro analysis. Results show that 5-HT increased PAI-1 expression in cultured murine proximal tubular epithelial cells (mProx cells) and SG improved it. The 5-HT-PAI-1 pathway is a promising new drug target for efforts against the progression of renal fibrosis.

ACKNOWLEDGMENTS

We thank Koki Takehara (Creative Partner Oboro) for support.

GRANTS

This work was supported by KAKEN-HI no. 23790931, MEXT, Japan (K. Doi), KAKEN-HI no. 24390212, MEXT, Japan (E. Noiri), and KAKEN-HI no. 25860288, MEXT, Japan (Y. Hamasaki).

DISCLOSURES

No conflicts of interest, financial or otherwise, are declared by the authors.

AUTHOR CONTRIBUTIONS

Author contributions: Y.H., K.D., R.M.-M., T.T., T.Y., T.S., M.N., and E.N. provided conception and design of research; Y.H., K.D., R.M.-M., E.O., D.K., and T.T. performed experiments; Y.H., K.D., R.M.-M., and T.T. analyzed data; Y.H., K.D., R.M.-M., E.O., D.K., T.T., and E.N. interpreted results of experiments; Y.H. and K.D. prepared figures; Y.H. and K.D. drafted manuscript; Y.H., K.D., and E.N. edited and revised manuscript; Y.H., K.D., R.M.-M., T.T., T.Y., T.S., M.N., and E.N. approved final version of manuscript.

REFERENCES

1. **Ataka K, Maruyama H, Neichi T, Miyazaki J, Gejyo F.** Effects of erythropoietin-gene electrotransfer in rats with adenine-induced renal failure. *Am J Nephrol* 23: 315–323, 2003.
2. **Chen CF, Yeh SU, Chien CT, Wu MS.** Renal response during acute unilateral ureteral obstruction in rats. *Neurourol Urodyn* 20: 125–137, 2001.
3. **Coresh J, Selvin E, Stevens LA, Manzi J, Kusek JW, Eggers P, Van Lente F, Levey AS.** Prevalence of chronic kidney disease in the United States. *JAMA* 298: 2038–2047, 2007.
4. **Doi K, Katagiri D, Negishi K, Hasegawa S, Hamasaki Y, Fujita T, Matsubara T, Ishii T, Yahagi N, Sugaya T, Noiri E.** Mild elevation of urinary biomarkers in prerenal acute kidney injury. *Kidney Int* 82: 1114–1120, 2012.
5. **Eddy AA, Fogo AB.** Plasminogen activator inhibitor-1 in chronic kidney disease: evidence and mechanisms of action. *J Am Soc Nephrol* 17: 2999–3012, 2006.
6. **Eto Y, Nitta K, Uchida K, Tsutsui T, Natori K, Kawashima A, Yumura W, Nihei H.** Anti-mitogenic effects of sarpogrelate in cultured rat mesangial cells. *Life Sci* 60: PL193–PL199, 1997.
7. **Go AS, Chertow GM, Fan D, McCulloch CE, Hsu CY.** Chronic kidney disease and the risks of death, cardiovascular events, and hospitalization. *N Engl J Med* 351: 1296–1305, 2004.
8. **Gonzalez J, Klein J, Chauhan SD, Neau E, Calise D, Nevoit C, Chaaya R, Miravete M, Delage C, Bascands JL, Schanstra JP, Buffin-Meyer B.** Delayed treatment with plasminogen activator inhibitor-1 decoys reduces tubulointerstitial fibrosis. *Exp Biol Med (Maywood)* 234: 1511–1518, 2009.
9. **Grewal JS, Mukhin YV, Garnovskaya MN, Raymond JR, Greene EL.** Serotonin 5-HT2A receptor induces TGF-β1 expression in mesangial cells via ERK: proliferative and fibrotic signals. *Am J Physiol Renal Physiol* 276: F922–F930, 1999.
10. **Ha H, Oh EY, Lee HB.** The role of plasminogen activator inhibitor 1 in renal and cardiovascular diseases. *Nat Rev Nephrol* 5: 203–211, 2009.
11. **Hamasaki Y, Doi K, Okamoto K, Ijichi H, Seki G, Maeda-Mamiya R, Fujita T, Noiri E.** 3-Hydroxy-3-methylglutaryl-coenzyme A reductase inhibitor simvastatin ameliorates renal fibrosis through HOXA13-USAG-1 pathway. *Lab Invest* 92: 1161–1170, 2012.
12. **Hara H, Kitajima A, Shimada H, Tamao Y.** Antithrombotic effect of MCI-9042, a new antiplatelet agent on experimental thrombosis models. *Thromb Haemost* 66: 484–488, 1991.
13. **Iizuka K, Hamaue N, Machida T, Hirafuji M, Tsuji M.** Beneficial effects of sarpogrelate hydrochloride, a 5-HT2A receptor antagonist, supplemented with pioglitazone on diabetic model mice. *Endocr Res* 34: 18–30, 2009.
14. **Kamijo A, Kimura K, Sugaya T, Yamanouchi M, Hikawa A, Hirano N, Hirata Y, Goto A, Omata M.** Urinary fatty acid-binding protein as a new clinical marker of the progression of chronic renal disease. *J Lab Clin Med* 143: 23–30, 2004.
15. **Kamijo A, Sugaya T, Hikawa A, Okada M, Okumura F, Yamanouchi M, Honda A, Okabe M, Fujino T, Hirata Y, Omata M, Kaneko R, Fujii H, Fukamizu A, Kimura K.** Urinary excretion of fatty acid-binding protein reflects stress overload on the proximal tubules. *Am J Pathol* 165: 1243–1255, 2004.
16. **Kanai H, Hiromura K, Kuroiwa T, Maezawa A, Yano S, Naruse T.** Role of serotonin in nephrotoxic serum nephritis in WKY rats. *J Lab Clin Med* 129: 557–566, 1997.
17. **Kasho M, Sakai M, Sasahara T, Anami Y, Matsumura T, Takemura T, Matsuda H, Kobori S, Shichiri M.** Serotonin enhances the production of type IV collagen by human mesangial cells. *Kidney Int* 54: 1083–1092, 1998.
18. **Kawano H, Tsuji H, Nishimura H, Kimura S, Yano S, Ukimura N, Kunieda Y, Yoshizumi M, Sugano T, Nakagawa K, Masuda H, Sawada S, Nakagawa M.** Serotonin induces the expression of tissue factor and plasminogen activator inhibitor-1 in cultured rat aortic endothelial cells. *Blood* 97: 1697–1702, 2001.

19. **Keith DS, Nichols GA, Gullion CM, Brown JB, Smith DH.** Longitudinal follow-up and outcomes among a population with chronic kidney disease in a large managed care organization. *Arch Intern Med* 164: 659–663, 2004.
20. **Kim DC, Jun DW, Kwon YI, Lee KN, Lee HL, Lee OY, Yoon BC, Choi HS, Kim EK.** 5-HT2A receptor antagonists inhibit hepatic stellate cell activation and facilitate apoptosis. *Liver Int* 33: 535–543, 2013.
21. **Kim W, Moon SO, Lee SY, Jang KY, Cho CH, Koh GY, Choi KS, Yoon KH, Sung MJ, Kim DH, Lee S, Kang KP, Park SK.** COMP-angiopoietin-1 ameliorates renal fibrosis in a unilateral ureteral obstruction model. *J Am Soc Nephrol* 17: 2474–2483, 2006.
22. **Kobayashi S, Satoh M, Namikoshi T, Haruna Y, Fujimoto S, Arakawa S, Komai N, Tomita N, Sasaki T, Kashihara N.** Blockade of serotonin 2A receptor improves glomerular endothelial function in rats with streptozotocin-induced diabetic nephropathy. *Clin Exp Nephrol* 12: 119–125, 2008.
23. **Kohler HP, Grant PJ.** Plasminogen-activator inhibitor type 1 and coronary artery disease. *N Engl J Med* 342: 1792–1801, 2000.
24. **Liu RM.** Oxidative stress, plasminogen activator inhibitor 1, and lung fibrosis. *Antioxid Redox Signal* 10: 303–319, 2008.
25. **Loskutoff DJ, Quigley JP.** PAI-1, fibrosis, and the elusive provisional fibrin matrix. *J Clin Invest* 106: 1441–1443, 2000.
26. **Mackensen-Haen S, Bader R, Grund KE, Bohle A.** Correlations between renal cortical interstitial fibrosis, atrophy of the proximal tubules and impairment of the glomerular filtration rate. *Clin Nephrol* 15: 167–171, 1981.
27. **Malyszko J, Malyszko JS, Pawlak D, Pawlak K, Buczko W, Mysliwiec M.** Hemostasis, platelet function and serotonin in acute and chronic renal failure. *Thromb Res* 83: 351–361, 1996.
28. **Matsuo S, Lopez-Guisa JM, Cai X, Okamura DM, Alpers CE, Bumgarner RE, Peters MA, Zhang G, Eddy AA.** Multifunctionality of PAI-1 in fibrogenesis: evidence from obstructive nephropathy in PAI-1-overexpressing mice. *Kidney Int* 67: 2221–2238, 2005.
29. **Morrissey JJ, Klahr S.** Effect of AT_2 receptor blockade on the pathogenesis of renal fibrosis. *Am J Physiol Renal Physiol* 276: F39–F45, 1999.
30. **Nangaku M.** Chronic hypoxia and tubulointerstitial injury: a final common pathway to end-stage renal failure. *J Am Soc Nephrol* 17: 17–25, 2006.
31. **Nath KA.** Tubulointerstitial changes as a major determinant in the progression of renal damage. *Am J Kidney Dis* 20: 1–17, 1992.
32. **Negishi K, Noiri E, Maeda R, Portilla D, Sugaya T, Fujita T.** Renal L-type fatty acid-binding protein mediates the bezafibrate reduction of cisplatin-induced acute kidney injury. *Kidney Int* 73: 1374–1384, 2008.
33. **Ninomiya T, Kiyohara Y, Kubo M, Tanizaki Y, Doi Y, Okubo K, Wakugawa Y, Hata J, Oishi Y, Shikata K, Yonemoto K, Hirakata H, Iida M.** Chronic kidney disease and cardiovascular disease in a general Japanese population: the Hisayama Study. *Kidney Int* 68: 228–236, 2005.
34. **Nonogaki K, Nozue K, Oka Y.** Increased hypothalamic 5-HT2A receptor gene expression and effects of pharmacologic 5-HT2A receptor inactivation in obese Ay mice. *Biochem Biophys Res Commun* 351: 1078–1082, 2006.
35. **Oda T, Jung YO, Kim HS, Cai X, Lopez-Guisa JM, Ikeda Y, Eddy AA.** PAI-1 deficiency attenuates the fibrogenic response to ureteral obstruction. *Kidney Int* 60: 587–596, 2001.
36. **Rasbach KA, Funk JA, Jayavelu T, Green PT, Schnellmann RG.** 5-Hydroxytryptamine receptor stimulation of mitochondrial biogenesis. *J Pharmacol Exp Ther* 332: 632–639, 2010.
37. **Remuzzi G, Benigni A, Remuzzi A.** Mechanisms of progression and regression of renal lesions of chronic nephropathies and diabetes. *J Clin Invest* 116: 288–296, 2006.
38. **Remuzzi G, Bertani T.** Pathophysiology of progressive nephropathies. *N Engl J Med* 339: 1448–1456, 1998.
39. **Risdon RA, Sloper JC, De Wardener HE.** Relationship between renal function and histological changes found in renal-biopsy specimens from patients with persistent glomerular nephritis. *Lancet* 2: 363–366, 1968.
40. **Saini HK, Takeda N, Goyal RK, Kumamoto H, Arneja AS, Dhalla NS.** Therapeutic potentials of sarpogrelate in cardiovascular disease. *Cardiovasc Drug Rev* 22: 27–54, 2004.
41. **Santana AC, Degaspari S, Catanozi S, Delle H, de Sa Lima L, Silva C, Blanco P, Solez K, Scavone C, Noronha IL.** Thalidomide suppresses inflammation in adenine-induced CKD with uraemia in mice. *Nephrol Dial Transplant* 28: 1140–1149, 2013.
42. **Sarnak MJ, Levey AS, Schoolwerth AC, Coresh J, Culleton B, Hamm LL, McCullough PA, Kasiske BL, Kelepouris E, Klag MJ, Parfrey P, Pfeffer M, Raij L, Spinosa DJ, Wilson PW.** Kidney disease as a risk factor for development of cardiovascular disease: a statement from the American Heart Association Councils on Kidney in Cardiovascular Disease, High Blood Pressure Research, Clinical Cardiology, and Epidemiology and Prevention. *Circulation* 108: 2154–2169, 2003.
43. **Seo JY, Park J, Yu MR, Kim YS, Ha H, Lee HB.** Positive feedback loop between plasminogen activator inhibitor-1 and transforming growth factor-beta1 during renal fibrosis in diabetes. *Am J Nephrol* 30: 481–490, 2009.
44. **Sole MJ, Madapallimattam A, Baines AD.** An active pathway for serotonin synthesis by renal proximal tubules. *Kidney Int* 29: 689–694, 1986.
45. **Tamagaki K, Yuan Q, Ohkawa H, Imazeki I, Moriguchi Y, Imai N, Sasaki S, Takeda K, Fukagawa M.** Severe hyperparathyroidism with bone abnormalities and metastatic calcification in rats with adenine-induced uraemia. *Nephrol Dial Transplant* 21: 651–659, 2006.
46. **Tamura M, Aizawa R, Hori M, Ozaki H.** Progressive renal dysfunction and macrophage infiltration in interstitial fibrosis in an adenine-induced tubulointerstitial nephritis mouse model. *Histochem Cell Biol* 131: 483–490, 2009.
47. **Tanaka T, Doi K, Maeda-Mamiya R, Negishi K, Portilla D, Sugaya T, Fujita T, Noiri E.** Urinary L-type fatty acid-binding protein can reflect renal tubulointerstitial injury. *Am J Pathol* 174: 1203–1211, 2009.
48. **Tanaka T, Noiri E, Yamamoto T, Sugaya T, Negishi K, Maeda R, Nakamura K, Portilla D, Goto M, Fujita T.** Urinary human L-FABP is a potential biomarker to predict COX-inhibitor-induced renal injury. *Nephron Exp Nephrol* 108: e19–e26, 2008.
49. **Trivedi H.** Cost implications of caring for chronic kidney disease: are interventions cost-effective? *Adv Chronic Kidney Dis* 17: 265–270, 2010.
50. **Uchida-Kitajima S, Yamauchi T, Takashina Y, Okada-Iwabu M, Iwabu M, Ueki K, Kadowaki T.** 5-Hydroxytryptamine 2A receptor signaling cascade modulates adiponectin and plasminogen activator inhibitor 1 expression in adipose tissue. *FEBS Lett* 582: 3037–3044, 2008.
51. **Ullmer C, Schmuck K, Kalkman HO, Lubbert H.** Expression of serotonin receptor mRNAs in blood vessels. *FEBS Lett* 370: 215–221, 1995.
52. **Verbeke M, Van de Voorde J, de Ridder L, Lameire N.** Beneficial effect of serotonin 5-HT2-receptor antagonism on renal blood flow autoregulation in cyclosporin-treated rats. *J Am Soc Nephrol* 10: 28–34, 1999.
53. **Xu J, Yao B, Fan X, Langworthy MM, Zhang MZ, Harris RC.** Characterization of a putative intrarenal serotonergic system. *Am J Physiol Renal Physiol* 293: F1468–F1475, 2007.
54. **Yamakawa J, Takahashi T, Itoh T, Kusaka K, Kawaura K, Wang XQ, Kanda T.** A novel serotonin blocker, sarpogrelate, increases circulating adiponectin levels in diabetic patients with arteriosclerosis obliterans. *Diabetes Care* 26: 2477–2478, 2003.
55. **Yamamoto T, Kajiya F.** Intravital videomicroscopy. *Methods Mol Med* 86: 119–128, 2003.
56. **Yamamoto T, Noiri E, Ono Y, Doi K, Negishi K, Kamijo A, Kimura K, Fujita T, Kinukawa T, Taniguchi H, Nakamura K, Goto M, Shinozaki N, Ohshima S, Sugaya T.** Renal L-type fatty acid–binding protein in acute ischemic injury. *J Am Soc Nephrol* 18: 2894–2902, 2007.
57. **Yanada M, Kojima T, Ishiguro K, Nakayama Y, Yamamoto K, Matsushita T, Kadomatsu K, Nishimura M, Muramatsu T, Saito H.** Impact of antithrombin deficiency in thrombogenesis: lipopolysaccharide and stress-induced thrombus formation in heterozygous antithrombin-deficient mice. *Blood* 99: 2455–2458, 2002.
58. **Yokoyama T, Kamijo-Ikemori A, Sugaya T, Hoshino S, Yasuda T, Kimura K.** Urinary excretion of liver type fatty acid binding protein accurately reflects the degree of tubulointerstitial damage. *Am J Pathol* 174: 2096–2106, 2009.
59. **Yokozawa T, Zheng PD, Oura H, Koizumi F.** Animal model of adenine-induced chronic renal failure in rats. *Nephron* 44: 230–234, 1986.
60. **Yuen PS, Dunn SR, Miyaji T, Yasuda H, Sharma K, Star RA.** A simplified method for HPLC determination of creatinine in mouse serum. *Am J Physiol Renal Physiol* 286: F1116–F1119, 2004.

and unseeded small intestinal submucosa grafts in a subtotal cystectomy model. *BJU Int.* 2006; **98**: 1100–5.
28 Atala A, Bauer SB, Soker S, Yoo JJ, Retik AB. Tissue-engineered autologous bladders for patients needing cystoplasty. *Lancet* 2006; **367**: 1241–6.
29 Fraser M, Thomas DF, Pitt E, Harnden P, Trejdosiewicz LK, Southgate J. A surgical model of composite cystoplasty with cultured urothelial cells: a controlled study of gross outcome and urothelial phenotype. *BJU Int.* 2004; **93**: 609–16.
30 Turner A, Subramanian R, Thomas DF *et al.* Transplantation of autologous differentiated urothelium in an experimental model of composite cystoplasty. *Eur. Urol.* 2011; **59**: 447–54.
31 Rodriguez LV, Alfonso Z, Zhang R, Leung J, Wu B, Ignarro LJ. Clonogenic multipotent stem cells in human adipose tissue differentiate into functional smooth muscle cells. *Proc. Natl. Acad. Sci. U.S.A.* 2006; **103**: 12167–72.
32 Tian H, Bharadwaj S, Liu Y *et al.* Myogenic differentiation of human bone marrow mesenchymal stem cells on a 3D nano fibrous scaffold for bladder tissue engineering. *Biomaterials* 2010; **31**: 870–7.
33 Oottamasathien S, Wang Y, Williams K *et al.* Directed differentiation of embryonic stem cells into bladder tissue. *Dev. Biol.* 2007; **304**: 556–66.
34 Kinebuchi Y, Johkura K, Sasaki K, Imamura T, Mimura Y, Nishizawa O. Direct induction of layered tissues from mouse embryonic stem cells: potential for differentiation into urinary tract tissue. *Cell Tissue Res.* 2008; **331**: 605–15.
35 Thomas JC, Oottamasathien S, Makari JH *et al.* Temporal-spatial protein expression in bladder tissue derived from embryonic stem cells. *J. Urol.* 2008; **180** (Suppl): 1784–9.
36 Levitt SB, Reda EF. Hypospadias. *Pediatr. Ann.* 1997; **17**: 48–9, 53–4, 57.
37 Santucci RA, Joyce GF, Wise M. Male urethral stricture disease. *J. Urol.* 2007; **177**: 1667–74.
38 Chen F, Yoo JJ, Atala A. Acellular collagen matrix as a possible "off the shelf" biomaterial for urethral repair. *Urology* 1999; **54**: 407–10.
39 Atala A, Guzman L, Retik A. A novel inert collagen matrix for hypospadias repair. *J. Urol.* 1999; **162**: 1148–51.
40 le Roux PJ. Endoscopic urethroplasty with unseeded small intestinal submucosa collagen matrix grafts: a pilot study. *J. Urol.* 2005; **173**: 140–3.
41 Raya-Rivera A, Esquiliano DR, Yoo JJ, Lopez-Bayghen E, Soker S, Atala A. Tissue-engineered autologous urethras for patients who need reconstruction: an observational study. *Lancet* 2011; **377**: 1175–82.
42 Feldman HA, Goldstein I, Hatzichristou DG, Krane RJ, McKinlay JB. Impotence and its medical and psychosocial correlates results of the Massachusetts Male Aging Study. *J. Urol.* 1994; **151**: 54–61.
43 Kwon TG, Yoo JJ, Atala A. Autologous penile corpora cavernosa replacement using tissue engineering techniques. *J. Urol.* 2002; **168**: 1754–8.
44 Fandel TM, Albersen M, Lin G *et al.* Recruitment of intracavernously injected adipose-derived stem cells to the major pelvic ganglion improves erectile function in a rat model of cavernous nerve injury. *Eur. Urol.* 2012; **61**: 201–10.

Editorial Comment

Editorial Comment to Regenerative medicine as a new therapeutic strategy for lower urinary tract dysfunction

This review focuses on regenerative medicine approaches to treating specific maladies of the bladder, urethral sphincter, urethra and penis, including the biological basis of regeneration and the history of regenerative medicine in the lower urinary system.[1]

Regeneration of tissues and organs is now within technological reach of modern medicine. With such advancements, substantial improvements to existing standards-of-care are very real possibilities. Actually, Chancellar *et al.* reported muscle-derived stem cells in 1997 in the first human clinical trial in North America for stress incontinence in women.[2] We also reported adiposed-derived regenerative cells in 2012 in the first human trial at Nagoya University in Japan for stress incontinence after prostatectomy.[3] The current clinical management approaches for lower urinary tract will be presented within the context of future directions, including cell-based regenerative therapies.

Tokunori Yamamoto M.D., Ph.D. and Momokazu Gotoh M.D., Ph.D.
Department of Urology, Nagoya University Graduate School of Medicine, Nagoya, Japan
toku@med.nagoya-u.ac.jp

DOI: 10.1111/iju.12173

Conflict of interest

None declared.

References

1 Sumino Y, Mimata H. Regenerative medicine as a new therapeutic strategy for lower urinary tract dysfunction. *Int. J. Urol.* 2013; **20**: 670–5.
2 Carr LK, Steele D, Steele S *et al.* 1-Year follow-up of autologous muscle-derived stem cell injection pilot study to treat stress urinary incontinence. *Int. Urogynecol. J. Pelvic Floor Dysfunct.* 2008; **19**: 881–3. doi: 10.1007/s00192-007-0553-z.
3 Yamamoto T, Gotoh M, Kato M *et al.* Periurethral injection of autologous adipose-derived regenerative cells for the treatment of male stress urinary incontinence: report of three initial cases. *Int. J. Urol.* 2012; **19**: 652–9.

16 Jiang J, Chen YQ, Zhu YK, Yao XH, Qi J. Factors influencing the degree of enhancement of prostate cancer on contrast-enhanced transrectal ultrasonography: correlation with biopsy and radical prostatectomy specimens. *Br. J. Radiol.* 2012; **85**: 979–86.
17 Wink M, Frauscher F, Cosgrove D *et al.* Contrast-enhanced ultrasound and prostate cancer; a multicentre European research coordination project. *Eur. Urol.* 2008; **54**: 982–92.
18 Halpern EJ. Contrast-enhanced ultrasound imaging of prostate cancer. *Rev. Urol.* 2006; **8** (Suppl 1): S29–37.
19 Madjar H. Contrast ultrasound in breast tumor characterization: present situation and future tracks. *Eur. Radiol.* 2001; **11** (Suppl 3): E41–6.
20 Caruso G, Ienzi R, Cirino A *et al.* Breast lesion characterization with contrast-enhanced US. Work in progress. *Radiol. Med.* 2002; **104**: 443–50.
21 van Esser S, Veldhuis WB, van Hillegersberg R *et al.* Accuracy of contrast-enhanced breast ultrasound for pre-operative tumor size assessment in patients diagnosed with invasive ductal carcinoma of the breast. *Cancer Imaging* 2007; **7**: 63–8.
22 Brazdzionyte J, Macas A. Bland-Altman analysis as an alternative approach for statistical evaluation of agreement between two methods for measuring hemodynamics during acute myocardial infarction. *Medicina (Kaunas).* 2007; **43**: 208–14.
23 Bland JM, Altman DG. Comparing methods of measurement: why plotting difference against standard method is misleading. *Lancet* 1995; **346**: 1085–7.
24 Halpern EJ, Rosenberg M, Gomella LG. Prostate cancer: contrast-enhanced us for detection. *Radiology* 2001; **219**: 219–25.
25 Villers A, Puech P, Mouton D, Leroy X, Ballereau C, Lemaitre L. Dynamic contrast enhanced, pelvic phased array magnetic resonance imaging of localized prostate cancer for predicting tumor volume: correlation with radical prostatectomy findings. *J. Urol.* 2006; **176**: 2432–7.
26 Eichelberger LE, Koch MO, Daggy JK, Ulbright TM, Eble JN, Cheng L. Predicting tumor volume in radical prostatectomy specimens from patients with prostate cancer. *Am. J. Clin. Pathol.* 2003; **120**: 386–91.

Editorial Comment

Editorial Comment to Contrast-enhanced transrectal ultrasonography: Measurement of prostate cancer tumor size and correlation with radical prostatectomy specimens

The identification of microvascular abnormalities related to tumor-associated neovascularity in prostate cancer represents an ideal biopsy target. Microvascular abnormalities have shown a clear association between microvascular density, and the presence of malignancy, stage and survival.[1] Contrast-enhanced transrectal ultrasonography (CEUS) improves the visualization of the vascular morphology–perfusing malignant lesions. We have already reported a diagnosis of renal cell carcinoma using CEUS.[2] CEUS improves the visualization of the vascular morphology–perfusing malignant lesions, and the targeted biopsy provides a significant benefit for the detection of high grade/high volume.[1] CEUS is a significantly more accurate imaging technique than conventional grayscale imaging for measuring prostate tumor size, especially for tumors with a diameter >10 mm, and this technique might be applicable in preoperative assessment of prostatic index tumor sizes in the present article.[3] CEUS improves the visualization of the vascular morphology–perfusing malignant lesions. In one of the applications to clinical treatment, CEUS enhances the diagnostic power of focal therapy and detects prostate cancer more efficiently than grayscale transrectal ultrasonography imaging. Furthermore, CEUS assesses post-high intensity focused ultrasound tissue destruction and provides accurate detection of tumor recurrence, which is a key element for follow up.[4] CETUS could be helpful for characterization of neoplastic microcirculation of prostate cancer, for preoperative localization of cancer-suspect areas, and for therapy guidance and management. Applying the real-time technique of CEUS, new possibilities for the evaluation, intervention and monitoring of the therapy of prostatic cancer lesions were made possible, as the method also comprised dynamic microperfusion.[5]

Tokunori Yamamoto M.D., Ph.D.
Department of Urology, Nagoya University Graduate School of Medicine, Nagoya, Japan
toku@med.nagoya-u.ac.jp

DOI: 10.1111/iju.12164

Conflict of interest

None declared.

References

1 Halpern EJ, Gomella LG, Forsberg F, McCue PA, Trabulsi EJ. Contrast enhanced transrectal ultrasound for the detection of prostate cancer: a randomized, double-blind trial of dutasteride pretreatment. *J. Urol.* 2012; **188**: 1739–45.
2 Aoki S, Hattori R, Yamamoto T *et al.* Contrast-enhanced ultrasound using a time-intensity curve for diagnosis of renal cell carcinoma. *BJU Int.* 2011; **108**: 349–54.
3 Qi TY, Chen YQ, Jiang J, Zhu YK, Yao XH, Qi J. Contrast-enhanced transrectal ultrasonography: measurement of prostate cancer tumor size and correlation with radical prostatectomy specimens. *Int. J. Urol.* 2013; **20**: 1085–91.
4 Rouvière O, Gelet A, Crouzet S, Chapelon JY. Prostate focused ultrasound focal therapy – imaging for the future. *Nat. Rev. Clin. Oncol.* 2012; **9**: 721–7.
5 Jung EM, Wiggermann P, Greis C *et al.* First results of endocavity evaluation of the microvascularization of malignant prostate tumors using contrast enhanced ultrasound (CEUS) including perfusion analysis: first results. *Clin. Hemorheol. Microcirc.* 2012; **52**: 167–77.

Hirosaki Med. J. 64(Suppl.) : S1—S3, 2013

PRETREATMENT OF RENAL SUPSCAPULAR ADMINISTRATION OF ADIPOSE TISSUE-DERIVED STEM CELLS AMELIORATE ISCHEMIA-REPERFUSION-INDUCED ACUTE KIDNEY INJURY

Tokunori Yamamoto, Funahashi Yasuto, Yoshihisa Mastukawa, Masashi Kato, Yasushi Yoshino, and Momokzu Gotoh

Abstract

Background

Acute renal ischemic injury (AKI) represents a major clinical problem with renal arterial clamp at partial nephrectomy. The use of therapy using adipose tissue-derived stem cells(ASCs) has been suggested as a potential modality to attenuate the ischemic renal damage.

Methods

We investigated the possible reno-protection of pretreatment of ASCs before and after in a rat ischemia-reperfusion (I-R) model of AKI. Twenty-four hours post-ischemia, blood flow in peritubular capillaries (PTC) was measured using intravital videomicroscopy.

Results

We demonstrated that ADRC therapy significantly reduced serum creatinine and BUN. Histological analysis further validated a significantly attenuated tubular damage. Intravital videomicroscopy and measurement of red blood cell velocity in peritubular capillaries showed ASCs-injected kidneys displayed significant hemodynamic improvement.

Conclusions

The subscapular administration of ASCs to the kidney attenuates I/R renal injury though anti-inflammation, anti-apotoyic effect and peritubular capillary microcirculation. The present study suggests that ASCs would be a useful tool in preventing ischemic kidney damage in the clinical setting.

Hirosaki Med. J. **64, Supplement** : S1—S3, 2013

Key words: ADIPOSE TISSUE-DERIVED STEM CELLS; ISCHEMIA-REPERFUSION-INDUCED ACUTE KIDNEY INJURY; RENAL PROTECT; CYTOKINES

Background

Previous studies have demonstrated that administration of mesenchymal stromal cells (MSCs) accelerates the recovery of tissue injury in several organs including heart, liver, neuron, and pancreas. Administration of bone marrow-derived stromal cells (BMSCs) has also been shown to protect the kidney from AKI induced by cisplatin, glycerol, and ischemia-reperfusion injury. Recently, it has been demonstrated that MSCs can be obtained from adipose tissue. Like BMSCs, adipose tissue-derived stromal cells (ASCs) have the potential to differentiate into various types of cells and tissues. Previous studies suggest that ASCs may have an advantage over BMSCs. Firstly, adipose tissue is abundant, and can be obtained repeatedly with minimal invasive procedure. Secondly, the number of stem cells in the fat is greater than that in the bone marrow. Lastly, in general ASCs grow faster than BMSCs.

In a previous study, we reported renoprotection on and low serum cultured and non cultured ASCs and a transplanted endothelial cell for folic acid[2] and cisplathin induced[5] AKIs and acute

Department of Urology, Nagoya University
Corresponding Author: Tokunoti Yamamoto,
Department of Urology, Nagoya University
Tel: 052-744-2985
Fax: 052-744-2319
Email: toku@med.nagoya-u.ac.jp

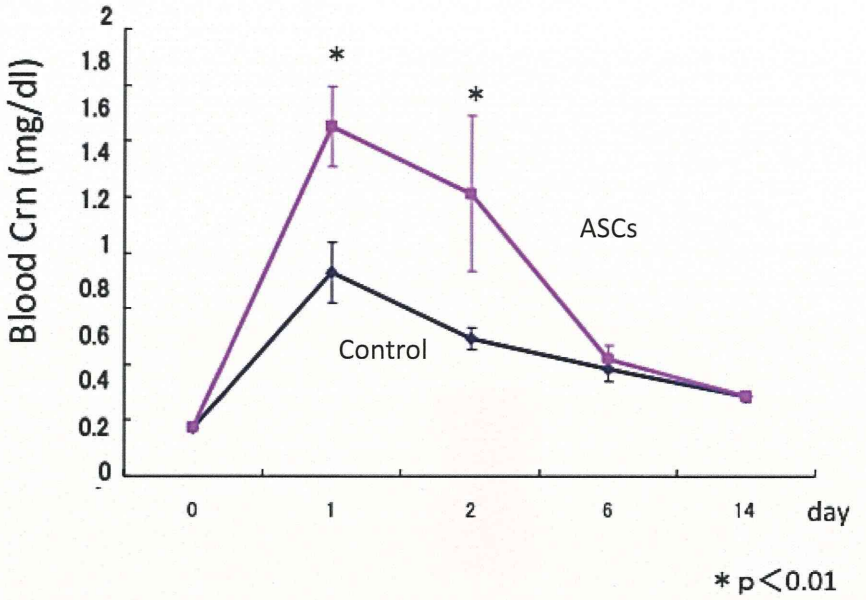

Fig 1. Renal function after the intravenous injection of low serum cultured human adipose tissue-derived stromal cells (hLASCs).

ischemia induced AKI[1] and. Aim is to cralify the renoprotection of ASCs for ischemia induced AKI.

MATERIALS AND METHODS

Culture conditions

The basal culture medium was prepared as previously described[4].

***In vivo* experimental subcapsular administration of hASCs**

Subcapsular injection of 2×106 of rat (r) -ASCs and control medium (Dulbecco's modified Eagle's medium, DMEM; Sigma-Aldrich) (each group n=6) was given to the left kidney of Acute kidney injury (AKI) rats. Blood samples were collected and blood urea nitrogen (BUN) and serum creatinine levels were measured by Mitsubishi Chemical Medience Co. Ltd (Tokyo, Japan). Rats were euthanized and renal cortical microcirculation was assessed using CCD video microscope[3] and kidney samples were taken for the study.

Morphological analysis

To evaluate tubulointerstitial injury, Hematoxin Eosin (HE) and periodic acid Schiff (PAS) stained kidney sections were analysed using a quantitative grading.

Renal function

Rats treated with control medium demonstrated a marked rise in BUN and serum creatinine and, r-ASCs further suppressed the increase of serum creatinine (Figure 1).

Tubular injury

Examination of PAS stained kidney sections taken from AKI rats treated with control medium showed severe tubular cell degenerative changes with necrosis and luminal casts. A r-ASCs greatly attenuated the tubular injury. The severity of the tubular damage, including tubular dilatation, degeneration and cast formation was scored. Treatment with r-ASCs resulted in significantly better scores than the control. In contrast, the r-ASCs-treated group failed to show significantly better scores than the control group.

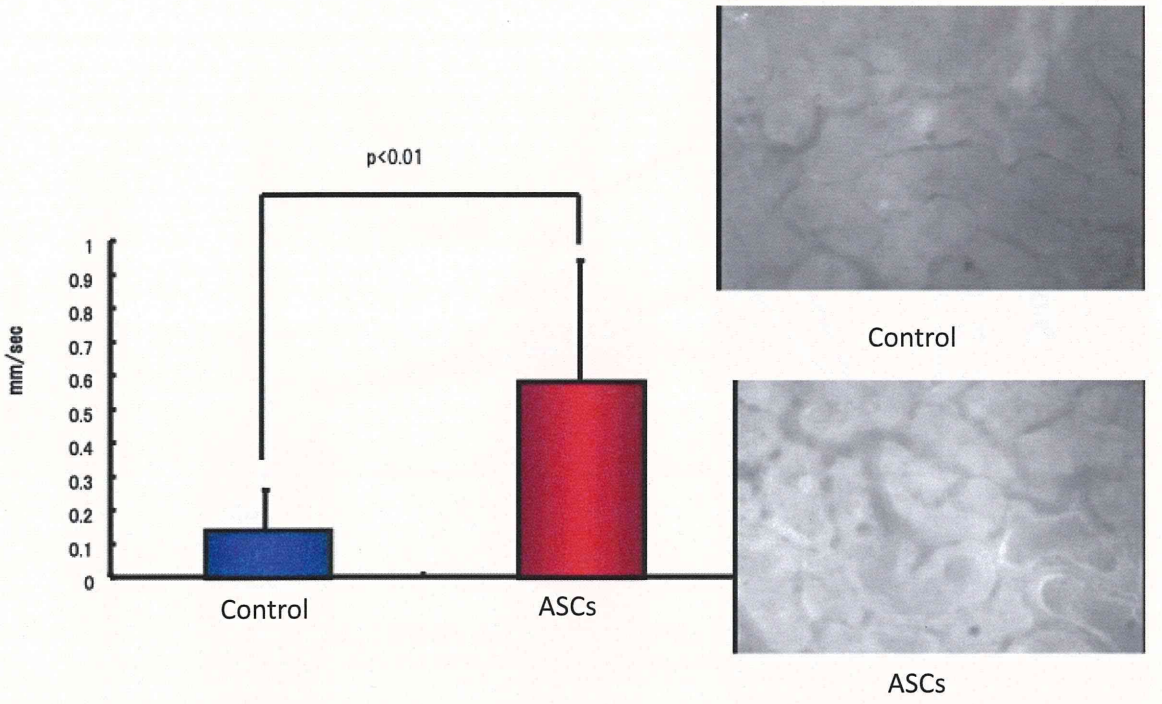

Fig 2. Renal cortical microcirculation. Velocity of the capillary blood flow and the capillary blood flow volume were significantly higher in AKI rats given subcapsular injection of hLASCs than those given the control medium.

Direct visualization of the renal cortical capillaries

The effects of r-ASCs on renal cortical microcirculation were examined by analyzing the direct images obtained with a CCD video microscope system. The blood flow velocity was significantly faster and the blood flow volume was greater in the r-ASCs group than in the control (Figure 2).

In conclusion, we demonstrate that subcapsular administration of r-ASCs protects the kidney via peritubulra microcircutaion from acute tubular injury.

References

1) Brodsky SV, Yamamoto T, Tada T, Kim B, Chen J, Kajiya F, Goligorsky MS. Endothelial dysfunction in ischemic acute renal failure: Rescue by transplanted endothelial cells. Am J Physiol Renal Physiol 2002;**282**:F1140-9.

2) Katsuno T, Ozaki T, Furuhashi K, Kim H, Yasuda K, Yamamoto T, Sato W, et al. Low serum cultured adipose tissue-derived stromal cells ameliorate acute kidney injury in rats. Cell Transplantation 2012 Sep 7. [Epub ahead of print]

3) Yamamoto T, Tada T, Brodsky SV, Tanaka H, Noiri E, Kajiya F, Goligorsky MS. Intravital videomicroscopy of peritubular capillaries in renal ischemia. Am J Physiol Renal Physiol 2002;**282**: F1150-5.

4) Iwashima S, Ozaki T, Maruyama S, Saka Y, Kobori M, Omae K, Yamaguchi H, et al. Novel culture system of mesenchymal stromal cells from human subcutaneous adipose tissue. Stem Cells Dev 2009;18(4):533-43.

5) Yasuda K, Ozaki T, Saka Y , Yamamoto T, Gotoh M , Ito Y, Yuzawa Y, Matsuo S Maruyama S, Autologous cell therapy for cisplatin induced acute kidney injury by using non-expanded adipose tissue derived cells Cytotherapy. 2012 2012 Oct;14(9):1089-100. doi: 10.3109/14653249.2012.693157. Epub 2012 Jun 25.

Cytotherapy, 2014; 16: 357–368

International Society for Cellular Therapy
ISCT

Rat adipose tissue-derived stem cells attenuate peritoneal injuries in rat zymosan-induced peritonitis accompanied by complement activation

HANGSOO KIM[1], MASASHI MIZUNO[1,2], KAZUHIRO FURUHASHI[1], TAKAYUKI KATSUNO[1], TAKENORI OZAKI[1], KAORU YASUDA[1], NAOTAKE TSUBOI[1], WAICHI SATO[1], YASUHIRO SUZUKI[1,2], SEIICHI MATSUO[1], YASUHIKO ITO[1,2] & SHOICHI MARUYAMA[1]

Division of Nephrology[1], Renal Replacement Therapy[2], Nagoya University Graduate School of Medicine, Nagoya, Japan

Abstract

Background aims. In patients receiving peritoneal dialysis, fungal or yeast peritonitis has a poor prognosis. In rat peritoneum with mechanical scraping, severe peritonitis can be induced by zymosan, a component of yeast (Zy/scraping peritonitis). Administration of rat adipose tissue-derived stromal cells (ASCs) potentially can improve several tissue injuries. The present study investigated whether rat ASCs could improve peritoneal inflammation in Zy/scraping peritonitis. *Methods.* Rat ASCs were injected intraperitoneally on a daily basis in rats with Zy/scraping peritonitis. *Results.* Peritoneal inflammation accompanied by accumulation of inflammatory cells and complement deposition was suppressed by day 5 after injection of rat ASCs. The peritoneal mesothelial layer in Zy/scraping peritonitis with rat ASC treatment was restored compared with the peritoneal mesothelial layer without rat ASC treatment. Injected rat ASCs co-existed with mesothelial cells in the sub-peritoneal layer. *In vitro* assays showed increased cellular proliferation of rat mesothelial cells combined with rat ASCs by co-culture assays, confirming that fluid factors from rat ASCs might play some role in facilitating the recovery of rat mesothelial cells. Hepatocyte growth factor was released from rat ASCs, and administration of recombinant hepatocyte growth factor increased rat mesothelial cell proliferation. *Conclusions.* Because the peritoneal mesothelium shows strong expression of membrane complement regulators such as Crry, CD55 and CD59, restoration of the mesothelial cell layer by rat ASCs might prevent deposition of complement activation products and ameliorate peritoneal injuries. This study suggests the therapeutic possibilities of intraperitoneal rat ASC injection to suppress peritoneal inflammation by restoring the mesothelial layer and decreasing complement activation in fungal or yeast peritonitis.

Key Words: *adipose-derived stromal cells, complement, membrane complement regulators, peritoneal dialysis, peritonitis*

Introduction

Peritoneal dialysis (PD) is an important renal replacement therapy. There are >196,000 patients with end-stage renal disease currently receiving PD therapy around the world (1). However, many patients must be withdrawn from PD therapy for various reasons (2,3). Impairment of peritoneal function is one of the main reasons for withdrawal from PD therapy. Peritoneal impairment is caused by the use of non-biocompatible PD fluid such as acid-base PD fluid and long-term exposure of the peritoneum to PD fluid. Peritonitis is another important and serious complication leading to withdrawal from PD therapy (3,4). Both conditions are associated with peritoneal tissue injuries and may be related to the development of lethal encapsulating peritoneal sclerosis (5). Such problems must be resolved to improve the prognosis of PD therapy in the future. In particular, fungal or yeast peritonitis is a serious infection in patients on PD (6) because fungal infection is known to be associated with a poor prognosis of peritonitis and can lead to the development of encapsulating peritoneal sclerosis (7,8). We previously reported that zymosan, a component of the yeast cell wall, can induce severe peritoneal inflammation in association with complement activation (9). Zymosan activates the complement activation system through the alternative pathway (10). We also reported that dysregulation of the complement activation system could be one factor associated with the development and augmented severity of

Correspondence: **Masashi Mizuno**, MD, PhD, Renal Replacement Therapy, Division of Nephrology, Nagoya University Graduate School of Medicine, Nagoya 466-8550, Japan. E-mail: mmizu@med.nagoya-u.ac.jp, masashinitjp@yahoo.co.jp

(Received 19 March 2013; accepted 22 October 2013)

http://dx.doi.org/10.1016/j.jcyt.2013.10.011

peritoneal injuries (9,11,12). Targeting the complement activation system might be one approach to control peritoneal injuries.

Studies using embryonic or pluripotent stem cells are valuable for analyzing pathologies, restoring injuries involving hematopoietic cells, neurons, muscle or cardiovascular tissue and developing new therapeutic agents (13–17). As the stem cells of mesenchymal tissues, mesenchymal stromal cells have shown great potential to repair tissue injuries in various animal disease models as alternatives to conventional therapies (18,19). Adipose tissue-derived stromal cells (ASCs) have an added advantage in that the cells can be harvested more easily and less invasively than bone marrow-derived mesenchymal stromal cells (20) and reportedly display immunomodulatory properties (21,22).

Using a rat peritonitis model induced by administration of zymosan after scraping the peritoneum (Zy/scraping peritonitis) (9), we showed that the initial inflammation in severe peritoneal injury was related to complement activation and that peritoneal inflammation of this peritonitis was enhanced by complement activation, supporting the poor prognosis of fungal PD peritonitis. In the present study, we investigated a suppressive effect of rat ASCs in peritoneal injuries, targeting regulation of the complement activation system in the rat Zy/scraping peritonitis model.

Methods

Animals

Male Sprague-Dawley rats weighing approximately 250 g (Japan SLC, Hamamatsu, Japan) were used. All animal experiments described here were carried out in accordance with the Animal Experimentation Guide of Nagoya University School of Medicine.

Reagents and antibodies

Zymosan A was purchased from Sigma-Aldrich (St Louis, MO, USA). Dianeal NPD-4 1.5% (Baxter, Tokyo, Japan) was used as a 1.5% neutral PD fluid (pH approximately 6.4). To investigate the distribution of rat membrane complement regulators (CRegs), anti-rat Crry (monoclonal antibody [mAb] TLD-1C11) was purchased from Hycult Biotechnology (Uden, the Netherlands), and anti-rat CD55 (mAb RDIII7) and anti-rat CD59 (mAb 6D1), which were kindly donated by Prof B. P. Morgan (Cardiff University), were characterized as described (23–25). Fluorescein isothiocyanate (FITC)-labeled rabbit anti-mouse immunoglobulin G (IgG) was purchased from MP Biomedicals (Santa Ana, CA, USA). To observe C3b and C5b–9 (membrane attack complex) deposition, we used FITC-rabbit anti-rat C3 (MP Biomedicals) and mouse anti-rat C9 (clone 2A1; Hycult Biotechnology), respectively, followed by incubation with FITC-goat anti-mouse IgG (MP Biomedicals). Naphthol AS-D chloroacetate ($C_{20}H_{16}ClNO_3$), N,N-dimethylformamide and Fast Blue BB Salt hemi(zinc chloride) salt ($C_{17}H_{18}N_3O_3Cl \cdot 1/2\ ZnCl_2$) were purchased from Sigma-Aldrich for an esterase reaction to detect neutrophils. To observe ED1-positive cells, mouse anti-rat monocyte (clone ED1) was purchased from BMA Biomedicals (Augst, Switzerland). To recognize mesothelial cells along the peritoneal surface, we used monoclonal mouse anti-human cytokeratin, which was cross-reactive against rat (Dako, Glostrup, Denmark).

Preparation and characterizations of rat ASCs and primary cell cultures of rat mesothelial cells

Rat ASCs were obtained from inguinal adipose tissue from male Sprague-Dawley rats and cultured in low serum culture medium according to previous reports (26,27). Briefly, in the cell culture of rat ASCs, the basal medium was a 3:2 mixture of Dulbecco's modified Eagle's medium (Nissui Pharmaceutical, Tokyo, Japan) and MCDB 201 medium (Sigma-Aldrich), supplemented with 1 mg/mL linoleic acid-albumin (Sigma-Aldrich), ITS liquid media supplement (100×) as 1:100 (v:v) (Sigma-Aldrich), 0.1 mmol/L ascorbic acid phosphate ester magnesium salt (Wako Pure Chemical Industries, Osaka, Japan), 50 U/mL penicillin and 50 μg/mL streptomycin (Gibco Life Technologies, Grand Island, NY, USA). Cells were cultured in culture medium containing 2% fetal bovine serum (FBS) (HyClone Laboratories, Logan, UT, USA) and 10 ng/mL human fibroblast growth factor 2 (PeproTech, Rocky Hill, NJ, USA).

Primary culture of mesothelial cells was obtained according to our previous report (11). Briefly, dissected omentum from a Sprague-Dawley rat was digested in 10 mL of 0.25% trypsin with 1 mmol/L ethylenediamine tetraacetic acid (Gibco Life Technologies) for 30 min at 37°C, followed by incubation for 1 h in fresh 0.25% trypsin with 1 mmol/L ethylenediamine tetraacetic acid at 37°C. The residual omentum fragment was removed from the cell suspension. M199 medium (Invitrogen, Carlsbad, CA, USA) with 10% FBS and a mixture of 50 U/mL penicillin and 50 μg/mL streptomycin (Gibco Life Technologies) as 1:100 (v:v) was added into the cell suspension and centrifuged at 1000 rpm for 5 min. The cell pellet was re-suspended in 4 mL of M199 medium with 10% FBS, plated into type 1 collagen-coated 6-cm dishes (IWAKI; Asahi Glass Co., Tokyo, Japan) and incubated at 37°C for 4 days. Characterization

of the primary culture of rat mesothelial cells was performed according to our previous report (11).

In vivo experimental protocol

Zymosan-induced peritonitis was developed by five daily intraperitoneal injections of 5 mg of zymosan mixed with PD fluid in rats with mechanical scraping of the right-sided parietal peritoneum (Zy/scraping peritonitis) as described in our previous report (9), with a small modification to use 1.5% PD fluid instead of 4.25% PD fluid. Each intraperitoneal injection was administered to rats with 6×10^6 rat ASCs/rat suspended in 3 mL of phosphate-buffered saline (PBS) filled with 1.5% PD fluid (3 mL on days 0 and 1 and 8 mL on days 2–4), as described in our previous reports (26–28). Rat ASCs was injected 2 h after injection of zymosan on day 0 and at the same time as zymosan injection on days 1–4. Rats were sacrificed on day 5 to obtain tissues. The experimental protocol is summarized in supplementary Figure 1.

Separately, to investigate the effects of rat ASCs for treatment of peritoneal injuries, rat ASCs or vehicle were intraperitoneally injected on days 1, 2, 3 and 4 after the first injection of zymosan was administered intraperitoneally as for Zy/scraping peritonitis. The experimental protocol and number of rats in each group are shown in supplementary Figure 2A.

Histologic analysis

The parietal peritoneum was cut into strips (approximately 5 × 20 mm for a strip; four strips were obtained from the right-sided parietal peritoneum with mechanical scraping). Two strips of the parietal peritoneum were randomly obtained and fixed in 10% buffered formalin and embedded in paraffin. Sections 4.5 μm thick were stained with hematoxylin-eosin for histologic analysis. The other two strips were used for immunohistochemistry analysis. To estimate peritoneal thickness as a marker of tissue damage to the parietal peritoneum, we randomly observed 20 fields/rat at ×100 magnification under light microscopy, using the mean value for that rat as the peritoneal thickness. To estimate total accumulated cells, the total number of infiltrated cells was counted in 20 fields at ×200 magnification under light microscopy. The total number of infiltrated cells was calculated as follows:

(Total count of infiltrated cells in sequential peritoneal areas under × 200 magnification)/20

Immunohistochemistry analysis

To investigate infiltrations of neutrophils and ED1-positive cells, paraffin-embedded sections were de-waxed in xylene, re-hydrated and washed in PBS. To detect neutrophils, we used the Fast Blue Salt method as an esterase reaction according to a previous report (29). Briefly, de-paraffinized sections were incubated in chloroacetate solution (5 mg naphthol AS-D in 1 mL of N,N-dimethylformamide mixed with 25 mg fast blue BB salt in 40 mL of PBS) overnight at 4°C in the dark. After rinsing with distilled water, slides were stained with Nuclear Fast Red counterstain (Vector Laboratories, Burlingame, CA, USA) to counterstain nuclei. To detect infiltrated ED1-positive cells, de-paraffinized sections were pre-treated with 0.3% H_2O_2 to block endogenous peroxidase and incubated in 10% normal goat serum (Jackson ImmunoResearch Laboratories, West Grove, PA, USA) in PBS to block nonspecific binding, followed by treatment with 10 mmol/L citrate buffer (pH 6.0) for antigen retrieval at 98°C for 30 min. De-paraffinized sections were also incubated with mAb ED1, followed by addition of conjugated goat anti-mouse IgG and horseradish peroxidase-labeled polymer (Histofine Simple Stain; Nichirei, Tokyo, Japan) as a secondary reagent. Development was performed using deaminobenzine tetrahydrochloride development reagent (Histofine Simple Stain). The number of neutrophils or ED1-positive cells was calculated using the following formula:

Number of neutrophils or ED1-positive cells = (total count of neutrophils or ED1-positive cells in 20 sequential peritoneal areas under × 200 magnification)/20

From snap-frozen peritoneal strips, sections 4.5 μm thick were prepared with a cryostat and fixed in acetone according to our previous report (9). To investigate recovery of the mesothelial cell layer along the injured peritoneum, frozen sections were first stained with anti-cytokeratin, followed by conjugated polyclonal goat anti-rabbit IgG antibody absorbed with untreated rat serum (1:1/v:v) and horseradish peroxidase-labeled polymer (Histofine Simple Stain) as a secondary reagent. Enzyme activity was finally detected using 3-amino-9-ethyl-carbozole (Dako). Recovery of the mesothelial cell layer in the injured peritoneum was estimated according to our previous report (30). Briefly, the length of cytokeratin-positive mesothelial cell layer in relation to the total length of the peritoneal surface was calculated under ×100 magnification as the proportion occupied by cytokeratin-positive cells. To investigate C3b deposition as a complement activation product, FITC-labeled anti-rat C3 was incubated on frozen sections. For detection of C5b–9 as another activation product, frozen sections were incubated with mouse anti-rat C9 followed by incubation with FITC-labeled goat anti-mouse IgG

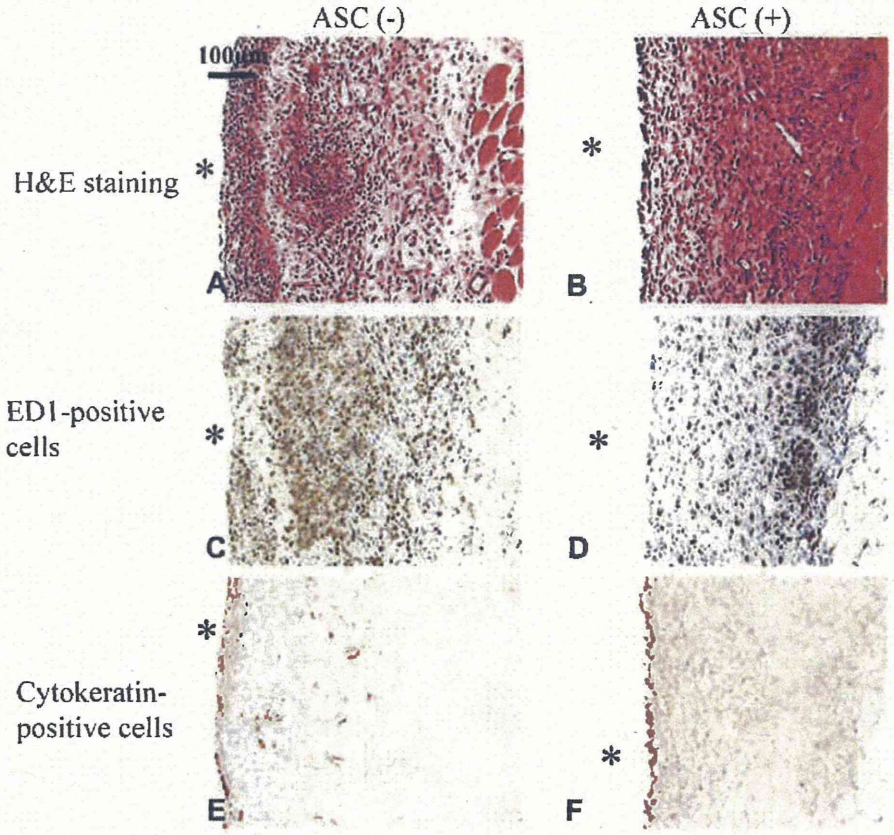

Figure 1. Microscopic findings in peritoneum treated with (ASC(+)) or without (ASC(−)) rat ASCs in Zy/scraping peritoneal peritonitis. (A, C, E) Micrographs show peritoneum without injection of rat ASCs in Zy/scraping peritonitis (ASC(−)). (B, D, F) Micrographs show rat ASC-injected rats (ASC(+)). Micrographs with hematoxylin-eosin (H&E) staining (A, B), ED1-positive cells (C,D) and distribution of cytokeratin in mesothelial cells (E, F). The thickness of peritoneum and accumulation of infiltrative cells are clearly decreased in rats treated with rat ASCs (ASC(+)) (B). Accumulation of ED1-positive cells is also reduced by rat ASCs (D). Cytokeratin-positive cells are apparent along the recovered peritoneal surface after injury in Zy/scraping peritonitis (F). *External face of the peritoneum. Scale bar is in upper left corner in (A).

absorbed with untreated rat serum (1:1/v:v). For C3b or C9 staining, we used normal rabbit serum or mouse serum as negative controls for antibodies. To score deposition of C3b or C5b−9 under ×200 magnification, a semi-quantitative scale was used: 0, negative result or only trace staining; 1, positive staining area <10% of total surface area; 2, positive staining area 10−30%; 3, positive staining area >30%. The mean value for degree of C3 or C5b−9 deposition from 20 fields was used. To examine the distribution of CRegs Crry, CD55 and CD59, mAbs (TLD-1C11, RDIII-7 and 6D1) were first incubated with the tissue sections, followed by FITC-labeled anti-mouse IgG. Distribution of the CRegs was also semi-quantified with the following scale: 0, negative; 1, positive staining area<20% of total surface area; 2, positive staining area 20% to <40%; 3, positive staining area 40% to <60%; 4, positive staining area 60% to <80%; 5, positive staining area >80%. The mean value for degree of CRegs expression from 20 fields was used.

Detecting distribution of 5-carboxy-fluorescein diacetate N-succinimidyl ester-labeled rat ASCs injected in rat Zy/scraping peritonitis

5-Carboxy-fluorescein diacetate N-succinimidyl ester (CFSE) was labeled on rat ASCs using a Cell Trace CFSE Cell Proliferation Kit (Molecular Probes, Eugene, OR, USA) in accordance with the instructions provided by the manufacturer. To observe the distribution of injected rat ASCs, 6×10^6 CFSE-labeled rat ASCs were injected on days 0 and 1 in the Zy/scraping peritonitis model. On day 3 after starting the experiment, rats were killed to harvest the peritoneum. Frozen sections from rats injected with CFSE-labeled rat ASCs were cut into 5-μm-thick sections and fixed with acetone for 10 min. First, to enhance the fluorescence signal, CFSE-labeled rat ASC tissues were incubated with anti-fluorescein/Oregon Green, goat IgG fraction (Molecular Probes) followed by FITC-labeled anti-goat IgG (Sigma-Aldrich). Second, to